

AMERICAN UNIVERSITY OF BEIRUT

STOCHASTIC SIMULATION OF THE SEISMIC RESPONSE
OF PILE SUPPORTED WHARF STRUCTURES
CONSIDERING INHERENT SOIL VARIABILITY

by
AHMAD ALI FAKIH

A Thesis
submitted in partial fulfillment of the requirements
for the degree of Master of Engineering
to the Department of Civil and Environmental Engineering
of the Maroun Semaan Faculty of Engineering and Architecture
at the American University of Beirut

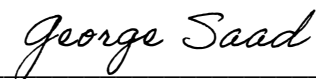
Beirut, Lebanon
January 2021

AMERICAN UNIVERSITY OF BEIRUT

STOCHASTIC SIMULATION OF THE SEISMIC RESPONSE
OF PILE SUPPORTED WHARF STRUCTURES
CONSIDERING INHERENT SOIL VARIABILITY

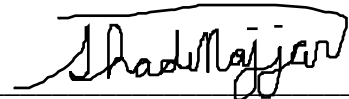
by
AHMAD ALI FAKIH

Approved by:



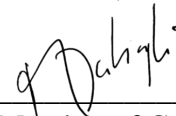
Dr. George Saad, Associate Professor
Civil and Environmental Engineering

Advisor



Dr. Shadi Najjar, Associate Professor
Civil and Environmental Engineering

Member of Committee



Dr. Mayssa Dabaghi, Assistant Professor
Civil and Environmental Engineering

Member of Committee

Date of thesis defense: January 26, 2021

AMERICAN UNIVERSITY OF BEIRUT

THESIS RELEASE FORM

Student Name: Fakih Ahmad Ali
 Last First Middle

I authorize the American University of Beirut, to: (a) reproduce hard or electronic copies of my thesis; (b) include such copies in the archives and digital repositories of the University; and (c) make freely available such copies to third parties for research or educational purposes:

- As of the date of submission
- One year from the date of submission of my thesis.
- Two years from the date of submission of my thesis.
- Three years from the date of submission of my thesis.



January 28, 2021

Signature

Date

(This form is signed & dated when submitting the thesis to the University Libraries ScholarWorks)

ACKNOWLEDGMENT

Thanks everyone!

ABSTRACT OF THE THESIS OF

Ahmad Ali Fakhri

for

Master of Engineering

Major: Structural Engineering

Title: Stochastic Simulation of the Seismic Response of Pile Supported Wharf Structures Considering Inherent Soil Variability

The aim of this research is to study the effect of inherent soil variability on the structural performance of laterally loaded pile supported wharf structures with an emphasis on assessing the current deterministic design practices by using an uncertainty quantification approach.

In order to represent the soil pile interaction, the p-y method was incorporated in two distinct modeling approaches: Deterministic approach where the upper and lower bounds p-multipliers were used to represent the current design practices and a probabilistic approach that treats some of the p-y parameters as random variables to represent the inherent uncertainty in soil which will in turn be transformed into stochastic structural response.

The outcomes of the first approach were assessed based on the probabilistic distributions drawn from the second approach. Additionally, a performance based design was done for both approaches where the deterministic demand to capacity ratios and their corresponding probabilities of failure were calculated.

Moreover, a sensitivity analysis for the correlation length was performed and its effect on the probability of failure was studied.

The results showed a compliance between both approaches in most cases except at the Operating Level Earthquake where the lower bound limit didn't cover the range of the probabilistic distribution. Also, it was shown that when the correlation length increases, the probability of failure decreases.

TABLE OF CONTENTS

| | |
|-----------------------------|---|
| ACKNOWLEDGEMENT | 1 |
| ABSTRACT..... | 2 |
| LIST OF ILLUSTRATIONS | 5 |
| LIST OF TABLES..... | 7 |

Chapter

| | |
|--|----|
| 1. INTRODUCTION..... | 8 |
| 1. Background..... | 8 |
| 2. Uncertainty of Soil Properties..... | 9 |
| 3. Problem and Objective..... | 10 |
| 4. Thesis Structure | 11 |
| 2. LITERATURE REVIEW..... | 12 |
| 1. Introduction..... | 12 |
| 2. Current Design Practices..... | 12 |
| 3. Inherent Variability of Soils..... | 14 |
| 4. Effect of Soil and Loading Uncertainty On Piles and Wharves | 15 |
| 5. Experimental Work..... | 17 |
| 6. Rock Dike Specifications..... | 19 |
| 7. Main Objective and Added Value..... | 20 |
| 3. METHODOLOGY..... | 21 |
| 1. Introduction..... | 21 |
| 2. P-y Method..... | 21 |

| | |
|--|-----------|
| 3. Pile Supported Wharf Model | 26 |
| 3.1. Model Properties and Specifications | 26 |
| 3.2. Deterministic Analysis | 32 |
| 3.3. Probabilistic Analysis | 33 |
| 3.4. MATLAB code | 36 |
| 4. RESULTS | 42 |
| 1. Introduction | 42 |
| 2. Deterministic Results | 42 |
| 2.1. Lower Bound Model Capacity | 42 |
| 2.2. Upper Bound Model Capacity | 44 |
| 2.3. Deterministic Demand vs. Capacity | 46 |
| 3. Stochastic Results | 48 |
| 3.1. Capacity | 49 |
| 3.2. Demand | 53 |
| 3.3. Correlation Length Sensitivity | 57 |
| 5. CONCLUSION AND RECOMMENDATIONS | 61 |
| 1. Conclusion | 61 |
| 2. Future Work | 63 |
| BIBLIOGRAPHY | 64 |
| APPENDIX | 66 |
| MATLAB Code | 66 |

ILLUSTRATIONS

Figure

| | |
|--|----|
| 1. Global shipping routes (Anon., 2012) | 8 |
| 2. Uncertainty of soil on different scales after (Vermeer, et al., 2013) | 10 |
| 3. Typical Wharf Cross-Section (source: The Port of Long Beach)..... | 11 |
| 4. Plastic Hinge Formation, Source: Port of Long Beach, 2015..... | 14 |
| 5. Lateral Resistance Correction Factor at different deflections (Diaz et al 1984)..... | 18 |
| 6. P-y Method | 22 |
| 7. K Value | 23 |
| 8. C1, C2 and C3 values | 24 |
| 9. Pile supported wharf structure model illustration..... | 28 |
| 10. Pile-deck connection detail (POLB)..... | 29 |
| 11. Wharf model on SAP2000..... | 29 |
| 12. Pile section modeled in SAP2000's section designer..... | 31 |
| 13. Random p-y curves with the friction angle as random variable | 34 |
| 14. Random p-y curves with the unit weight as random variable..... | 34 |
| 15. Probability distribution histogram | 38 |
| 16. p-y multilinear data in .\$.2k text file format..... | 40 |
| 17. Push-over curve for the lower bound model..... | 43 |
| 18. Hinging sequence for the lower bound model | 44 |
| 19. Push-over curve for the upper bound model..... | 45 |
| 20. Hinging sequence for the upper bound model | 45 |
| 21. Deterministic Results at DMF=1.5 | 48 |
| 22. Probabilistic Distribution of Horizontal Deck Displacements at OLE Level | 49 |

| | |
|--|----|
| 23. Jumps in the lateral deck displacement due to different hinging sequences | 50 |
| 24. Probabilistic Distribution of Horizontal Deck Displacements at CLE Level | 51 |
| 25. Probabilistic Distribution of Horizontal Deck Displacements at DE Level | 52 |
| 26. Max shear force distribution in the first 2 piles at OLE | 52 |
| 27. Max shear force distribution in the first 2 piles at CLE..... | 53 |
| 28. Max shear force distribution in the first 2 piles at DE..... | 53 |
| 29. Max El-Centro Horizontal Deck Displacement Demand at x1g, x2g and x3g | 54 |
| 30. Comparison of deterministic and probabilistic results at DMF=1.5..... | 55 |
| 31. Comparison of deterministic and probabilistic results at DMF=1.9..... | 56 |
| 32. Deterministic Results at DMF=1.9 | 56 |
| 33. Lateral Deck Displacement at $\theta_x = 10$ and $\theta_x = 100$ for different limit states while θ_y fixed at 1.5..... | 58 |
| 34. Lateral Deck Displacement at $\theta_y = 0.5$ and $\theta_y = 5$ for different limit states while θ_x fixed at 10..... | 59 |
| 35. The variation of the probability of failure as a function of the vertical correlation length under x2g El-Centro at OLE limit..... | 60 |
| 36. The variation of the probability of failure as a function of the vertical correlation length under x3g El-Centro at OLE limit..... | 60 |

TABLES

Table

| | |
|---|----|
| 1. Strain limits for the different design level (POLB) | 30 |
| 2. Plastic Hinge Length, Seismic Design of Wharf and Piers (ASCE, 2014) | 31 |
| 3. Mean and Standard Deviation for the soil layers in degrees | 35 |
| 4. The total "Distances Matrix" containing the 36 sub-matrices | 37 |
| 5. Random variables matrix | 39 |
| 6. Deterministic demand and capacity horizontal deck displacements | 46 |
| 7. Demand to capacity ratios for the lower bound model | 47 |
| 8. Demand to capacity ratios for the upper bound model | 47 |
| 9. Probability of failure based on 2000 simulation at DMF=1.5 | 55 |

CHAPTER 1

INTRODUCTION

1. Background

The continuous nature of trading and transportation between countries is essential to maintain a sustainable world economy that can satisfy the needs of all countries. All the international trading routes in the world are connected through man-made structures that act as stations for imports and exports. Unfortunately, many of these stations can be structurally vulnerable to natural hazards such as earthquakes that can interrupt the continuity of the international trading; thus, imposing huge costs on the economy.



According to the European Community of Ship-owners Association (European Community of Ship-owners Association, n.d.) around 80% of world trade in goods is carried by the international shipping industry in which exports and imports are executed on wharf structures. This shows the investment importance of wharf stations and the huge economic loss if a possible failure occurs. Throughout history, many wharves

around the world were damaged by earthquakes such as the Port of Kobe, Japan, during the 1995 earthquake (Esper & Tachibana, 1998) and Port Blair, S. Andaman Island, 2004 earthquake (Kaushik & Jain, 2007) among many others. For the sake of mitigating such a potential lateral damage, wharf structures performance should be further analyzed and improved.

For the sake of improving the structural performance, engineers aim to identify the sources of uncertainty involved and then translate these uncertainties into probabilistic models that can predict possible outcomes.

In the case of pile supported wharf structures, one can pinpoint several sources of uncertainties ranging from the uncertainty in the seismic demand to the methodology of developing lateral p-y springs and the uncertainties regarding the placement of the sloping rock dike. But this thesis intends to focus mainly on the uncertainty arisen from the spatial variability of soil properties. While the current design practices are deterministic by nature, probabilistic models aim to assess the performance of the latter design methodology.

2. Uncertainty of Soil Properties

Being a naturally occurring material formed through centuries of erosion and sedimentation, soil can exhibit a high amount of variability through its volume which translates into considerable level of uncertainty when dealing with soil-structure interaction problems; thus, emerges the importance of assessing the geotechnical reliability of our structures through stochastic models. Figure 2 shows the different levels of spatial randomness in soils from the microscopic to the geotechnical and geological scales.

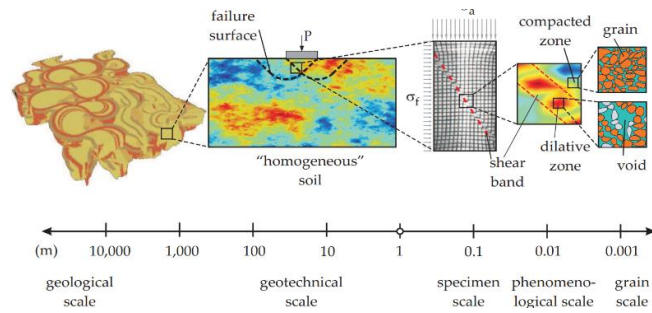


Figure 2 Uncertainty of soil on different scales after (Vermeer, et al., 2013)

Through the continuous process of testing the mechanical properties of soils, it's possible for researchers to develop the statistical parameters for different soil types that can be updated and improved over time. This probabilistic process is called "Bayesian Updating" and it was first developed by Thomas Bayes in the 18th century. Knowing the average and the standard deviation for the different soil properties and how these properties correlate and vary through the spatial dimensions will allow engineers to create probabilistic models that can predict the probabilities of all the possible soil behaviors under certain excitations; thus, we can manage and control the associated uncertainty and finally assess the risks involved.

3. Problem and Objective

Wharf structures usually consist of a deck supported on piles that rest tangentially and normally on a sloping soil mass (Figure 3). Soil by nature exhibits a high level of uncertainty where its parameters vary rapidly across the spatial dimensions of its mass. This uncertainty in soil can lead to uncertainty in the predicted structural behavior.

The available practical design codes for wharf structures depend on certain bound limits that should theoretically contain the true solution, but the amount of uncertainty arising from the variation of the soil layers properties can be substantial. This leads to a large range between upper and lower bounds in deterministic studies that may either be not safe enough or not economic enough and thus the need for a probabilistic

uncertainty quantification analysis emerges. As an attempt to do the latter, this study proposes creating a pile-supported wharf structure model resting on sand while treating uncertain soil parameters that affects the structural response as random variables. The model is expected to yield different probabilistic random distributions of the structural behavior that are to be compared with the deterministic approach so that the reliability and performance of the structure can be assessed.

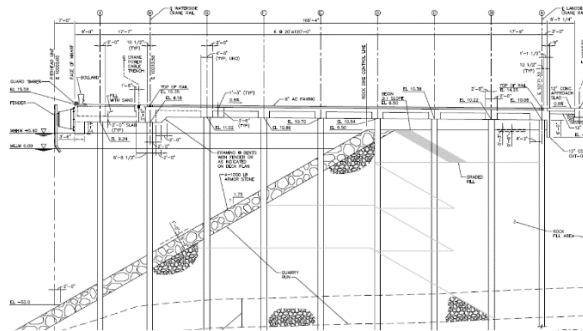


Figure 3 Typical Wharf Cross-Section (source: The Port of Long Beach)

4. Thesis Structure

The thesis consists of 5 chapters including the current one. Chapter 2 will present a literature review about the previous works done in this area of research.

After that, the methodology and the modeling techniques will be discussed in chapter 3 then the outcomes and results will be shown and investigated in chapter 4.

Ultimately, the corresponding conclusions will be drawn-out and summarized in chapter 5.

CHAPTER 2

LITERATURE REVIEW

1. Introduction

This chapter will first present a summary of the resources related to current practices involved with designing pile supported wharf structures and then moves to the various experimental and theoretical work in the area related to the latter and the uncertainties involved with the soil-structure interaction. The content of this chapter can be distributed over several sections as follows:

- Current Design Practices
- Inherent Variability of Soils
- Effect of Soil and Loading Uncertainty on Piles and Wharves
- Experimental Work
- Rock Dike Specifications

2. Current Design Practices

The analysis and design of Pile supported wharf structures is considered a soil-structure interaction problem where stresses are induced by the pile on the soil and vice versa.

The soil-pile interaction generally consists of two phenomena: Inertial and Kinematic interactions.

Inertial interaction can be described as the stresses induced by the superstructure's mass and inertia on the piles and the soil due to lateral forces (seismic condition). (Port of Long Beach Wharf Design Criteria, 2015) and the ASCE Standards

on The Seismic Design of Wharves and Piers (ASCE, 2014) provides the guidelines for the practical design of pile supported wharves. These guidelines adopt the p-y method for the lateral analysis of piles where the soil is represented by nonlinear springs (this method will be discussed more in the later sections). But due to uncertainties associated with that method, upper and lower bounds p-multipliers are introduced. The latter mentioned references suggests using values of 0.3 and 2 as lower and upper p-multitplier bounds respectively when dealing with a slope/embankment/dike system and for a level-ground configuration it's recommended to use 0.8 and 1.25 bounds. The p-multipliers are supposed to be used for slopes between 1.5H:1V and 1.75H:1V.

Kinematic interaction is due to the permanent deformations in the deep levels of the soil that happens because of the lateral spreading where the inability of the piles to match this free field motion of the soil will induce additional stresses. As suggested by the POLB, the free field motion dominates mainly at the deeper levels and is considered to occur beyond 10 pile diameters from the ground surface while the inertial interactions will dominate within that range. According to POLB, kinematic analysis could be avoided if deformations at different levels of ground motions using Newmark Sliding Block method comply with the allowable displacements.

2-dimensional push-over analysis is recommended by the design guidelines for all wharf structures. The push-over curve shall include the points that represent the yield displacement, and the displacement limits corresponding to the Operating Level Earthquake (OLE), Contingency Level Earthquake (CLE) and Code-level Design Earthquake (DE). These limit states are simulated by the use of plastic hinges at different depths along the pile (Figure 4). The corresponding limit strains for steel and reinforced concrete are presented in the POLB criteria.

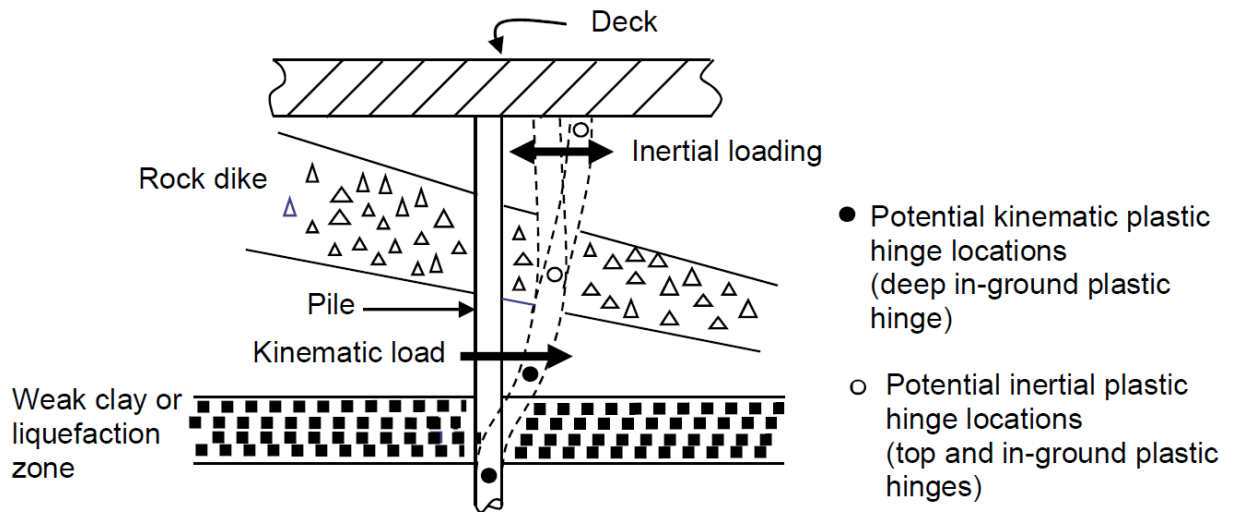


Figure 4 Plastic Hinge Formation, Source: Port of Long Beach, 2015.

3. Inherent Variability of Soils

Being a natural material, soils are considered to be among the most uncertain aspects in structural engineering.

In their book, Fenton and Griffiths (Fenton & Griffiths, 2008) presented probabilistic methods for dealing with various geotechnical problems among which is the deep foundations or piles. It is stated that the soil-pile profile is to be divided into a series of sections where each section is represented by a spring with a random stiffness and this can be considered a 1-dimensional random finite element method. The spring stiffness in our case will be defined by the p-y relationship that contains several soil parameters. One or more of these parameters will be treated as a random variable depending on the effect of their variability on the p-y curves. The soil parameters will have a vertical and horizontal spatial correlation with a correlation length θ . According to Fenton and Griffiths, Correlation length is the distance within which points are significantly correlated.

(Fan & Liang, 2013) examined the effect of the variation of the correlation length for various clay parameters on the probability of failure and found out that this

probability is mostly affected by the variation of the undrained shear strength's correlation length. No similar research was found for sands but it's expected that the friction angle will be the major affecting parameter and this will be proven in the later sections.

The soil variability can be modeled through a stochastic model that renders each element as a random variable having probabilistic distributions for its material parameters. This process is called Random Finite Element Method (RFEM) and it's elaborated in details by (Fenton & Griffiths, 2008). The other method is to use discrete springs that exhibits nonlinear empirical p-y relationships and the parameters involved can be treated as random variables. Due to its simplicity and low computational costs, practical engineers mostly use the p-y method. Therefore the latter method will be adopted in this research. The probabilistic model used in this research will be discussed in details later in the methodology section.

4. Effect of Soil and Loading Uncertainty On Piles and Wharves

In their case study article, (R. Gregory, et al., 2012) expressed the importance of understanding and implementing the sources of uncertainty in our models in order to mitigate the seismic risk in port structures. While the possible sources of uncertainty could be many, we will mainly be focusing on two types in this literature review: Seismic uncertainty which can be represented by fragility curves and inherent soil variability which is the main topic of this research.

(Talukder & M Lye, 2008) performed a probabilistic analysis using Monte Carlo simulations to study the effect of variation of soil and loading parameters on the probability of failure of a laterally loaded pile. It was found that the variation of the

lateral loading is the most influential parameter on the behavior of the pile. This study was performed on a single pile but a more complex behavior could emerge when dealing with multiple piles.

(Chanda, et al., 2019) studied the effects of uncertainty of shear strength parameters ϕ and c_u on the structural response and period of a building supported on piles under static and dynamic loading. In sandy soils, the effect of variability was found to be significant in dynamic analysis but marginal under static loading and it was considerable in both types of analyses for clayey soils. In both soils, the fundamental period of the structure was marginally affected. They also found out that using a fixed base or the code proposed SSI design guidelines could lead to unsafe design while considering nonlinear soil-pile interaction on the other hand is more conservative. In the above researches, the behavior of the pile itself was considered elastic. For a better understanding of the actual behavior, it's more realistic to include plastic hinges or use a nonlinear pile model.

(Hamid Heidary-Torkamani, et al., 2013) created a nonlinear finite difference model and examined the seismic sensitivity of wharf structures due to uncertainty in geotechnical properties using tornado diagrams and by treating the soil as continuum. It was found that the uncertainty in the friction angle of the rock fill contributes the most to the sensitivity of the differential settlement and the uncertainty in the permeability of the sand fill highly affects the sensitivity of lateral displacement.

(Mirfattah & Lai, 2015) also studied the effects of uncertainty in soil properties on the probabilistic seismic performance of pile-supported wharves. A stochastic finite difference model was created and it was shown that the uncertainties in geotechnical properties significantly affects the seismic response of wharf structures. Additionally, the variation in characteristics of ground motions with the same intensity was more

influential to the response of pile-supported wharves than that of the variation in system properties.

(Lei Su, et al., 2019) performed a seismic fragility analysis for pile-supported wharves. Seismic fragility analysis indicates the probability of exceeding a damage limit state for a given structure subjected to a seismic excitation. A pushover analysis is performed through gradually increasing the lateral displacement of wharf deck thus increasing the concrete strain gradually at which the slight, moderate, and extensive damage states can be identified and the bound limits of demand parameters associated with different damage states are obtained. Additionally, they showed that the piles with the shorter free length are more vulnerable to suffer seismic damage. Furthermore, they studied the sensitivity of the system against permeability where the dike exhibits the most significant sensitivity due to its highly permeable nature.

(Su, Wan, Dong, M. Frangopol, & Ling, 2019) published another research with similar model as the one above but this time they studied the effect of the soil pile interaction on the seismic behavior of the structure. It was found that soil pile interaction have substantial effect on the push-response and the seismic fragility of the wharf especially under extensive damage state.

(Mohsen Soltani & Rouhollah Amirabadi, 2018) examined the effect of uncertainty in the direction of earthquakes on a pile supported wharf structure using fragility curves and came out with critical angles for the different damage states.

5. Experimental Work

Some experiments were performed by previous researchers to further understand the behavior of piles under lateral loads.

(Diaz, et al., 1984) performed a full scale test on laterally loaded piles in sloping rock fill for the sake of designing a wharf constructed at the Port of Los Angeles that features vertical pre-stressed concrete piles and came out with a lateral resistance correction factor that reduces the ultimate resistance of soil to accommodate for the effect of the sloping ground. (Figure 5)

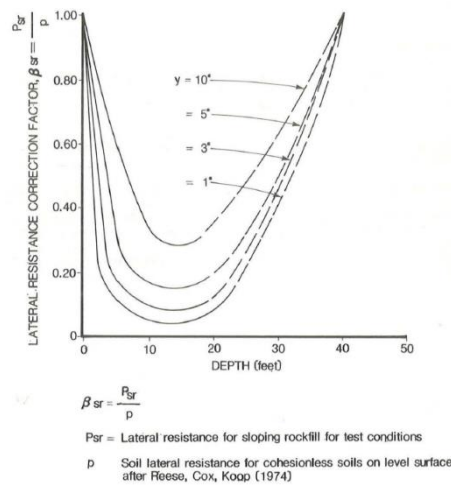


Figure 5 Lateral Resistance Correction Factor at different deflections (Diaz et al 1984)

(Kawamata, 2009) conducted a series of full scale lateral load tests on piles as a part of his PhD dissertation in order to better understand the behavior of pile supported wharf structures in several soil layers including a rock fill dike. His aim was to compare his experiments to the numerical p-y models where he showed that the p-y method underestimates the ultimate lateral resistance but accurately captures the deflection and rotation profiles of the pile. It was shown that the rock fill layer has a considerable effect on the system behavior. Finally, several uncertain soil parameters that can affect the structural behavior were discussed and it was suggested to add the concept of interlocking to the p-y methodology to capture the particulate mechanism in the rock fill layer.

(Folke Møller & Christiansen, 2011) performed downscaled tests on laterally loaded mono-piles in dry and saturated sand under static and cyclic loading. They also created different numerical models using the p-y method and the finite element method. It was shown that the ultimate bearing capacity prescribed by the theoretical p-y curves was underestimated for static loading while in cyclic loading the stiffness and ultimate resistance is improved with more cycles.

6. Rock Dike Specifications

Wharf structures usually rest on a sloping soil that is exposed to water tides. These continuous tides can damage and erode the slope which necessitate the addition of a rock dike layer to protect and retain the underlying soil.

There is scarce information in literature on the behavior of rock dike under lateral forces which adds to the uncertainty involved when analyzing wharf structures. In practice, the rock-dike is treated as a cohesionless soil having a friction angle of 38-39° (Martin, 2005). While this is not an accurate representation of the actual behavior, the upper and lower p-multiplier bounds are supposed to encompass the actual solution.

In (Diaz, et al., 1984)'s full scale experiment, a relation between the lateral resistance of cohesionless soils on a horizontal surface and the resistance of rock dike at a slope is presented (Figure 5). At great depths the slope didn't have much effect and at intermediate depths, the slope had a reasonable effect which is expected but at shallow depths, the effect is reversed. Meaning that near the surface, the rock dike still has resistance downslope similar to a cohesionless soil on horizontal slope. i.e: At the surface level, the resistance (P) is supposed to be null according to the cohesionless sand API model assumed for the rock dike, however the actual experiment has shown some resistance caused by the rock dike itself. Diaz et al attributed this effect to the fact

that each rock has to “climb” over its neighboring particles in order for it to move which generates some additional resistance even at the surface level.

In Kawamata’s experiments (Kawamata, 2009), the resulted p-y curves were compared with those from the upper-bound model where the rock dike was treated as a cohesionless soil. The experiment showed a high resistance caused by the rock dike that even surpassed the upper bound limit for the cohesionless soil from the API model. Kawamata attributed this “higher than expected” resistance by the rock dike to several factors related to the size of the soil particles relative to the pile diameter where the large rock particles will need to “climb” over each other which will increase the soil resistance even at the surface level. Another factor is the compression imposed by single rocks on other rocks which also increases the resistance. The current cohesionless soil model used in practice don’t take these new effects into consideration.

For an accurate representation of the rock dike, a pseudo-cohesive finite element model should be incorporated as done by (J. McCullough & E. Dickenson, 2004), but this is out of the scope of this thesis.

7. Main Objective and Added Value

The previous works done covered various aspects of uncertainties in the structural analysis of pile supported wharves. But the added value of this thesis is to incorporate the methodology of using upper and lower bounds in the deterministic soil-pile interaction analysis and put it side by side with a probabilistic approach that quantifies the uncertainty in soils. Both methods will be subjected to a performance based design that will yield a deterministic demand to capacity ratio on one hand, and a probability of failure on the other. Additionally, the effect of the vertical and horizontal correlation lengths in the probabilistic approach will be studied.

CHAPTER 3

METHODOLOGY

1. Introduction

This chapter will explain all the elements involved with the analysis, modeling and obtaining the results. The methodology will focus on the following key elements:

- P-y Method: clarifying the concept of the method and identifying the equations to be used for the lateral analysis of piles.
- Pile Supported Wharf Model: showing the overall model details and the numerical modeling techniques adopted along with the performance based analysis.
- Uncertainty Quantification: presenting the probabilistic method used and the code based stochastic model created.
-

2. P-y Method

The p-y method suggests that the pile-soil interaction can be simulated by a series of springs each having an elasto-plastic stiffness depending on their depth so that the deeper parts of the soil will carry more load due to the better confinement (Figure 6).

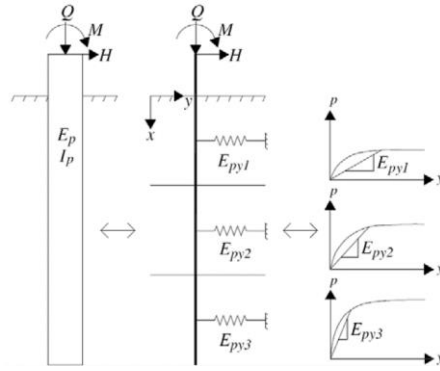


Figure 6 P-y Method

A laterally loaded pile can be modeled as a beam on Winkler foundation having the following differential equation:

$$E_p I_p \cdot \frac{d^4 y}{dx^4} + Q \cdot \frac{d^2 y}{dx^2} - E_{py} \cdot y = 0 \quad (1)$$

Where $E_p I_p$ is the flexural rigidity

Q is the axial force

y is the lateral displacement

E_{py} is the modulus of subgrade reaction

A finite difference software such as LPILE (M. Isenhower & Wang, 2013) can solve this differential equation and calculate the resulting shear, moment and deflection.

This method models the pile as an elastic section. In order to study the plastic formation in the pile's section, plastic hinges shall be incorporated in the model by the use of software such as SAP2000.

The theoretical expression of the p-y curves in sands as suggested by O'Neill et al (O'Neill & Murchison, 1983) and adopted by the API code:

$$p = \eta \cdot A \cdot p_u \cdot \tanh\left(\frac{k \cdot z}{A \cdot p_u \cdot y}\right) \quad (2)$$

Where $\eta = 1$ for circular sections.

k is the initial modulus of subgrade reaction and can be calculated from Figure 7.

z is the depth below ground surface.

P_u is the ultimate bearing capacity.

p is the resistance of the soil $A = 0.9$ for cyclic loading.

y is the displacement. $A = \left(3.0 - 0.8 \frac{H}{D} \right) \geq 0.9$ for static loading.

A is the empirical adjustment factor.

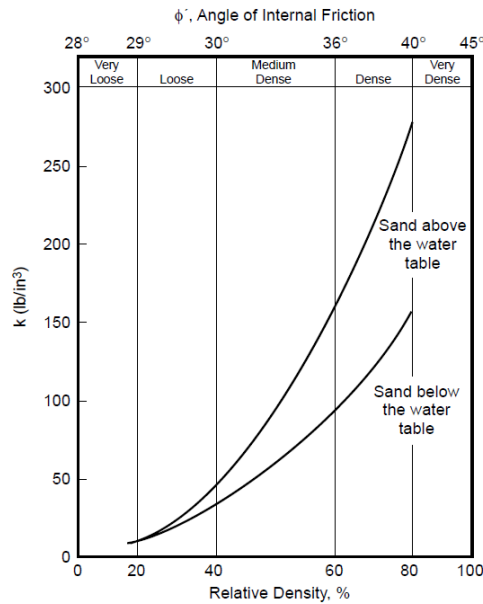


Figure 7 K Value

The ultimate bearing capacity P_u is the smallest between these two ultimate resistance caused by the 2 modes of failure: The wedge failure P_{us} and the flow failure P_{ud} .

$$P_{us} = (C_1 \times H + C_2 \times D) \times \gamma \times H \quad (3)$$

$$P_{ud} = C_3 \times D \times \gamma \times H \quad (4)$$

Where D is the diameter, H is the depth, γ is the unit weight.

C_1, C_2, C_3 =Coefficients determined from Figure 8(They can be also determined by other equations adopted in the code based model).

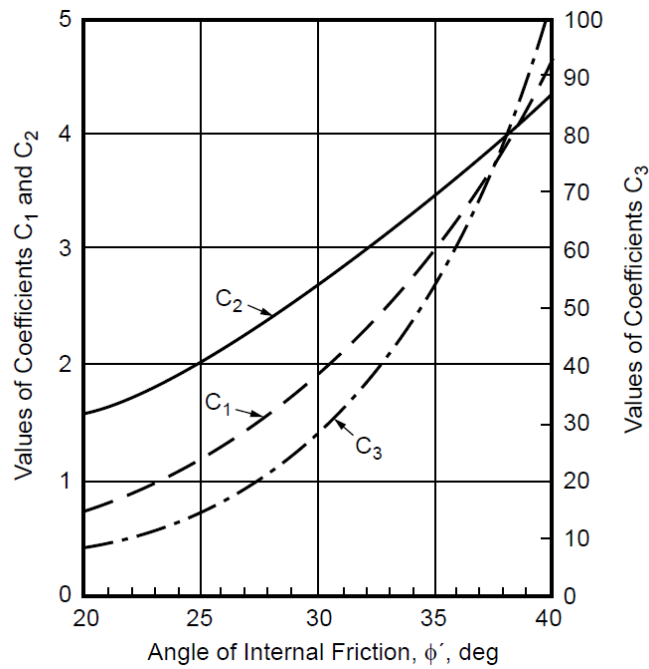


Figure 8 C_1 , C_2 and C_3 values

In typical wharf structures, most piles are placed in a sloping ground. This will reduce the lateral resistance of the soil from the down-slope's side. (Mathukkumaran, et al., 2008) adjusted the API p-y sand formula above to accommodate the effect of the sloping ground by multiplying P_u by a reduction factor "R". Note that this formula was derived based on a pile at the tip of the slope.

$$p = \eta \cdot R \cdot A \cdot p_u \cdot \tanh\left(\frac{k \cdot z}{A \cdot R \cdot p_u} \cdot y\right) \quad (5)$$

Where

$$R = 0.74 + 0.0378 \left(\frac{Z}{D}\right) - 0.6315(S); R \leq 1 ; \quad (6)$$

Z is the depth in meters;

D is the diameter of the pile;

S is the slope angle in radians (applicable from 0.5 to 0.66).

But in reality, piles in wharf structures can be anywhere along the slope. This will not only reduce the lateral resistance from the downslope's side but also will

increase it in the other direction due to more soil accumulating upslope and thus more confinement.

The technical manual of the software “LPile” by Ensoft (M. Isenhower & Wang, 2013) suggests some modifications on the initial p-y equations based on the earth pressure theory to accommodate for the effect of slope in both directions.

- P-y relation in the downslope direction:

$$(p_u)_{sa} = \gamma \cdot H \cdot \left[\frac{K_0 \cdot H \cdot \tan(\emptyset) \cdot \sin(\beta)}{\tan(\beta - \varphi) \cdot \cos(\alpha)} \cdot (4D_1^3 - 3D_1^2 + 1) + \frac{\tan(\beta)}{\tan(\beta - \varphi)} \cdot (b \cdot D_2 + H \tan(\beta) \cdot \tan(\alpha) \cdot D_2^2) + K_0 \cdot H \cdot \tan(\beta) \cdot (\tan(\emptyset) \cdot \sin(\beta) - \tan(\alpha)) \cdot (4D_1^3 - 3D_1^2 + 1) - K_A \cdot b \right] \quad (7)$$

Where

$$D_1 = \frac{\tan(\beta) \tan(\theta)}{\tan(\beta) \tan(\theta + 1)}; \quad (8)$$

$$D_2 = 1 - D_1; \quad (9)$$

$$K_A = \cos(\theta) \cdot \frac{\cos(\theta) - \sqrt{\cos^2(\theta) - \cos^2(\emptyset)}}{\cos(\theta) + \sqrt{\cos^2(\theta) - \cos^2(\emptyset)}}; \quad (10)$$

H is the depth;

b is the pile's diameter; $\alpha = \frac{\varphi}{2}$

θ is the slope's angle; $\beta = 45^\circ + \frac{\varphi}{2}$

- P-y relation in the upslope direction:

$$(p_u)_{sa} = \gamma \cdot H \cdot \left[\frac{K_0 \cdot H \cdot \tan(\emptyset) \cdot \sin(\beta)}{\tan(\beta - \varphi) \cdot \cos(\alpha)} \cdot (4D_3^3 - 3D_3^2 + 1) + \frac{\tan(\beta)}{\tan(\beta - \varphi)} \cdot (b \cdot D_4 + H \cdot \tan(\beta) \cdot \tan(\alpha) \cdot D_4^2) + K_0 \cdot H \cdot \tan(\beta) \cdot (\tan(\emptyset) \cdot \sin(\beta) - \tan(\alpha)) \cdot (4D_3^3 - 3D_3^2 + 1) - K_A \cdot b \right] \quad (11)$$

$$\text{Where } D_3 = \frac{\tan(\beta) \cdot \tan(\theta)}{1 - \tan(\beta) \cdot \tan(\theta)} \quad (0.12); \quad D_4 = 1 + D_3. \quad (13)$$

Some piles might not be influenced by the slope, according to (Mezazigh & Levacher, 1998), the effect of the slope will be negligible for piles that are more than 6D or 7D away from it.

The downslope equation will be adopted for the seawards analysis in our model.

Finally, the rock-dike is treated as a cohesionless soil having a higher mean friction angle (Martin, 2005). The rock-dike friction angle used is going to be equal to 41°.

3. Pile Supported Wharf Model

In this section, the different elements and properties used in creating the wharf model will be presented. SAP2000 software is used for the sake of simulating the structural behavior and the soil-structure interaction.

3.1. Model Properties and Specifications

The wharf model adopted in this research will consist of a 30 cm thick deck supported on six 22.36 meters long reinforced concrete piles having 65 cm diameter and spaced at 5.5 meters. The piles will penetrate 2 layers of soil, the first layer is 1.5 m thick rock dike with 41 degrees friction angle followed by a sand layer for the rest of the depth with an average angle of internal friction equal to 35 degrees. The structure is illustrated in Figure 9.

As recommended by the (Port of Long Beach Wharf Design Criteria, 2015), the deck-pile connection shouldn't be treated as entirely rigid. A strain penetration length L_{sp} should be assigned at the top of the pile through the deck section followed by a rigid link connected to the center of gravity of the deck (Figure 10). The strain penetration length is defined as follows:

$$l_{sp} = 0.1f_{ye}d_{bl} \quad (14)$$

Where,

l_{sp} = Strain penetration length (in.);

d_{bl} = The diameter of the dowel reinforcement (in.);

f_{ye} = Expected yield strength of the longitudinal reinforcement (ksi).

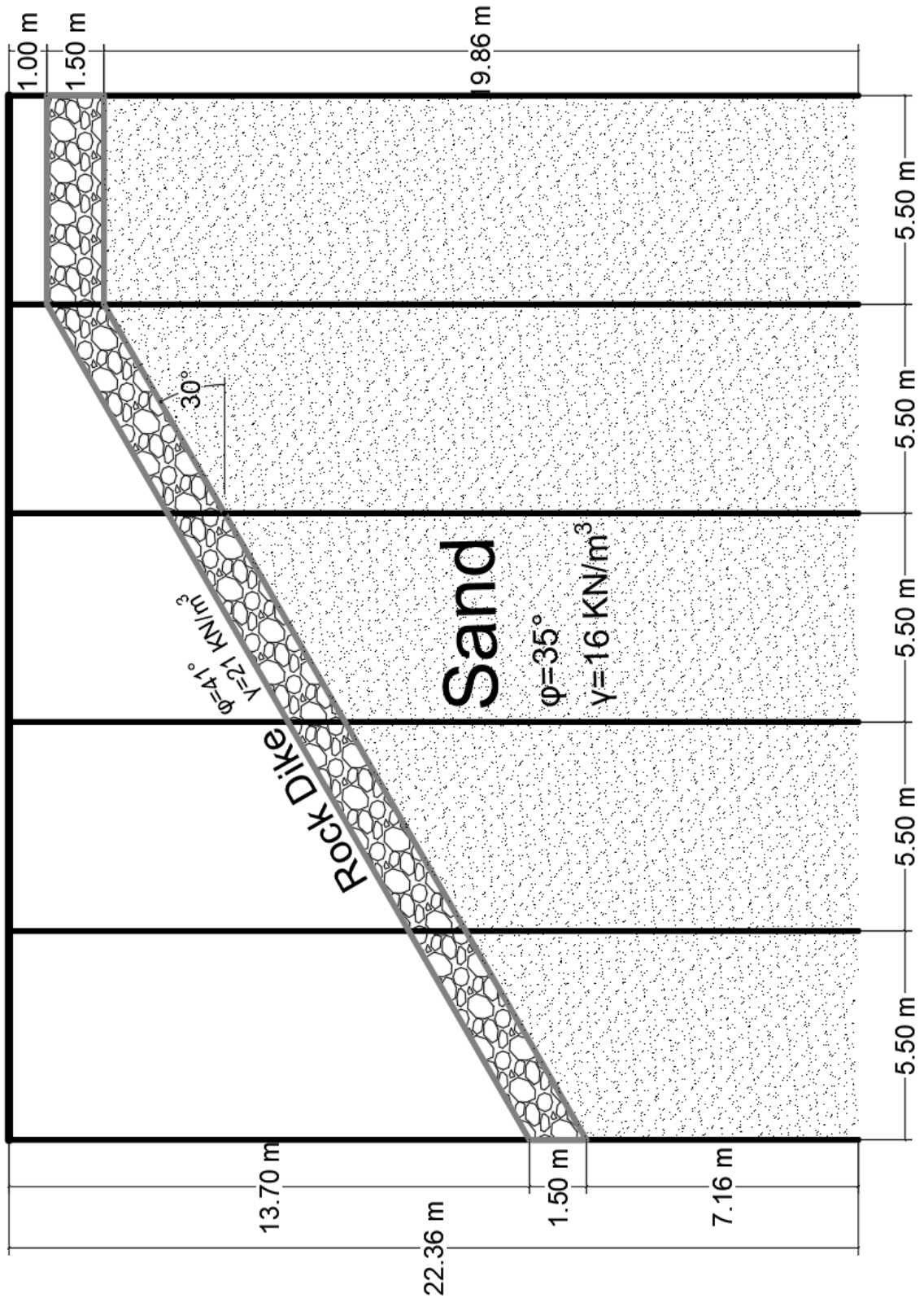


Figure 9 Pile supported wharf structure model illustration

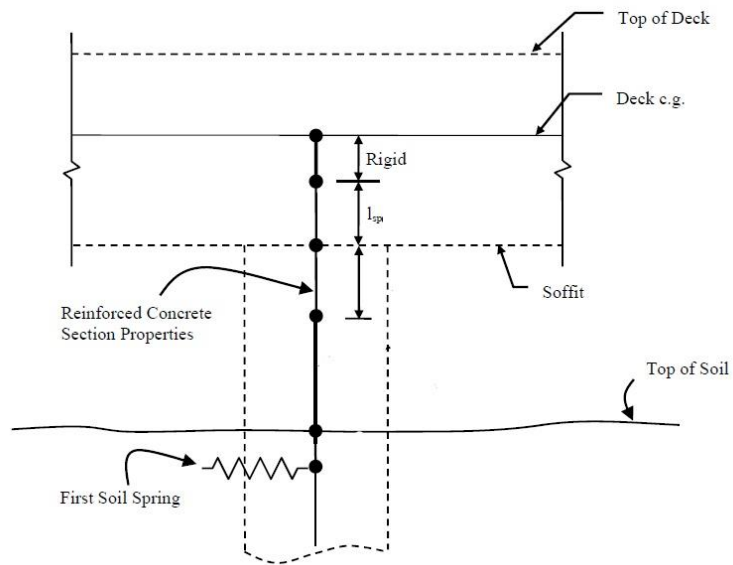


Figure 10 Pile-deck connection detail (POLB)

A 2 dimensional model is created using the software CSI SAP2000 where the deck and the piles are modeled as frame elements (Figure 11). The soil is simulated through a series of 2-point multilinear links having one point connected to the pile and the other point fixed. The link's multilinear property is defined by the p-y non-linear curve discussed in the previous section.

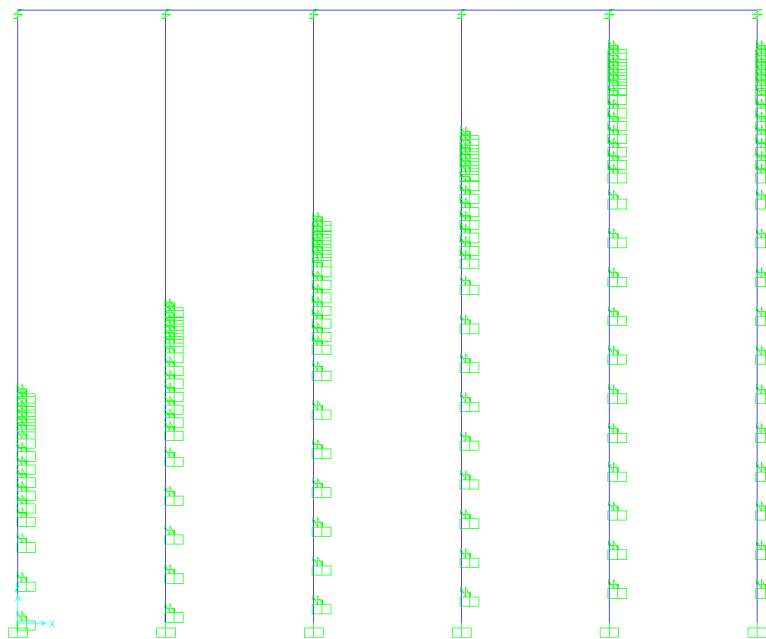


Figure 11 Wharf model on SAP2000

As shown in the previous figure, the spacing of the soil springs is dense near the surface where it's expected to obtain relatively large deformations and then they gradually become further apart as they go deeper into the soil where very little displacements are expected to occur. This way of distributing the soil springs enhance the computational efficiency while at the same time maintains accurate results.

Plastic hinges are assigned to the pile in order to capture the nonlinear behavior of the soil under the push-over analysis and thus specify the different stages at which the strain limits occur. 2 plastic hinges are assigned in each pile as shown in the literature review, "Current Design Practices" section. One hinge will be allocated at the top of the pile and the other in-ground at the location of the maximum moment. The corresponding strain limits as recommended by (Port of Long Beach Wharf Design Criteria, 2015) and adopted by the Standards on The Seismic Design of Wharves and Piers (ASCE, 2014) are presented in Table 1.

Table 1 Strain limits for the different design level (POLB)

| Component Strain | | Design Level | | |
|----------------------------------|---|----------------------------|---|---|
| | | OLE | CLE | DE |
| Solid Concrete Pile ^a | Top of pile hinge concrete strain | $\varepsilon_c \leq 0.005$ | $\varepsilon_c \leq 0.005 + 1.1\rho_s \leq 0.025$ | No limit |
| | In-ground hinge concrete strain | $\varepsilon_c \leq 0.005$ | $\varepsilon_c \leq 0.005 + 1.1\rho_s \leq 0.008$ | $\varepsilon_c \leq 0.005 + 1.1\rho_s \leq 0.012$ |
| | Deep In-ground hinge (>10D _p) concrete strain | $\varepsilon_c \leq 0.008$ | $\varepsilon_c \leq 0.012$ | No limit |
| | Top of pile hinge reinforcing steel strain | $\varepsilon_s \leq 0.015$ | $\varepsilon_s \leq 0.6\varepsilon_{smd} \leq 0.06$ | $\varepsilon_s \leq 0.8\varepsilon_{smd} \leq 0.08$ |
| | In-ground hinge prestressing steel strain | $\varepsilon_p \leq 0.015$ | $\varepsilon_p \leq 0.025$ | $\varepsilon_p \leq 0.035$ |
| | Deep In-ground hinge (>10D _p) prestressing steel strain | $\varepsilon_p \leq 0.015$ | $\varepsilon_p \leq 0.025$ | $\varepsilon_p \leq 0.050$ |

The length of the plastic hinges can be calculated from the formulas in Table 2.

Table 2: Plastic Hinge Length, Seismic Design of Wharf and Piers (ASCE, 2014)

| Connection type | L_p at deck (in.) |
|-----------------------------------|--|
| Steel pipe piles | |
| Embedded pile | $0.5D$ (see Section 7.4.3.3) |
| Concrete plug | $0.30f_{yc}d_b$ |
| Isolated shell | $0.30f_{yc}d_b + g$ |
| Welded embed | $0.5D$ (See Section 7.4.2.4) |
| Welded dowels | NA |
| Prestressed concrete piles | |
| Pile buildup | $0.15f_{yc}d_b \leq L_p \leq 0.3f_{yc}d_b$ |
| Extended strand | $0.2f_{pye}d_{st}$ |
| Embedded pile | $0.5D$ (see Section 7.4.2.1) |
| Dowelled | $0.25f_{yc}d_b$ |
| Hollow dowelled | $0.2f_{yc}d_b$ |
| External confinement | $0.30f_{yc}d_b$ |
| Isolated interface | $0.25f_{yc}d_b$ |
| Other connections | |
| Pinned connection | NA |
| Batter pile | See Section 7.4.4.2 |

Note: Table uses English units. Metric equivalent is not provided.

The Moment curvature diagram and the P-M interaction curves are extracted using SAP2000's section designer while treating the pile section as a fiber model as shown in Figure 12.

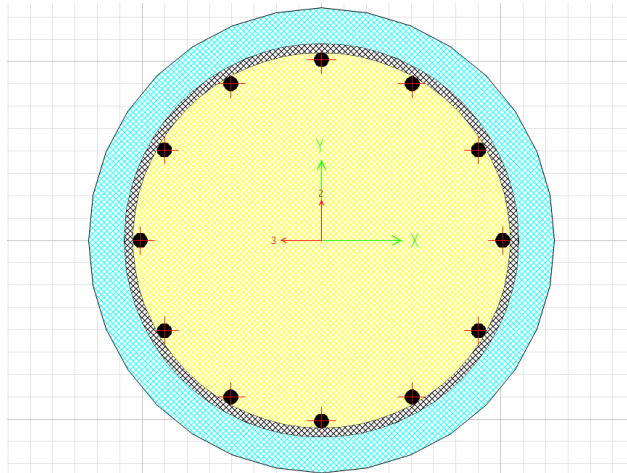


Figure 12 Pile section modeled in SAP2000's section designer

The effective inertia I_{eff} of the piles is calculated as recommended by (ASCE, 2014) using the yield moment M_y , reduction coefficient at yield ϕ_y and the concrete modulus of elasticity E_c :

$$M_y = 264 \text{ Kn.m}$$

$$\phi_y = 0.0051$$

$$E_c = 24855578 \text{ Kn/m}^2$$

$$I_{gross} = 8.65e-3 \text{ m}^3$$

$$I_{eff} = \frac{M_y}{\phi_y \cdot E_c} = 2.0735e^{-3} \text{ m}^4$$

$$\text{Pile Stiffness Modifier} = \frac{I_{eff}}{I_{gross}} = 0.24$$

The load cases consists of:

- The structure's self-weight.
- Distributed live load on the deck of 20 KN/m.
- The push-over lateral loading imposed at the deck level.
- El-Centro Time history ground motion at 3 scales: 1g, 2g and 3g where g is the gravitational constant.

3 design levels are used as mentioned before: the Operating Level Earthquake (OLE), Contingency Level Earthquake (CLE) and Code-level Design Earthquake (DE). The displacement at each level is to be recorded under the push-over analysis and the time history ground motion to obtain the displacement capacities and demands respectively.

There will be two types of analyses: Deterministic and Probabilistic.

3.2. Deterministic Analysis

The first aspect of the comparative analysis is setting up the deterministic models which represent the current design practices. 2 deterministic models are created

representing the lower and upper bounds where the soil resistance “p” in the p-y curves is multiplied by 0.3 and 2 respectively. After running the models, the displacement and shear capacities at the different design levels are extracted in addition to the displacement demands at the different time history scales.

3.3.Probabilistic Analysis

In order to quantify the uncertainty involved, probabilistic analysis is required along with a Monte-Carlo simulation. The first step is to identify the random variables that have the biggest influence on the variability of the results. The 2 main mechanical properties of sands are the friction angle and the unit weight. A preliminary code is created using MATLAB to identify the most influential parameter by generating lognormally distributed random p-y curves using either the friction angle or the unit weight as a random variable. Figure 13 shows the a lognormal distribution of the p-y curves while treating the friction angle as random variable having a mean of 36.68 degrees and a standard deviation of 3.14 degrees and Figure 14 shows the same results but while treating the unit weight as a random variable having a mean of 19 KN/m³ and standard deviation of 0.76 KN/m³. It’s clear from the latter figures that the variation of the friction angle causes far more divergence in the results in terms of the initial slope and the ultimate resistance than that of the unit weight where in in the latter, the initial slope for all the generated random p-y curves is the same and the ultimate resistance has a relatively tight variance range. So for the sake of simplicity, only the friction angle will be adopted as the main random variable in our probabilistic model as it’s the biggest source of uncertainty that can influence the structural behavior of sands.

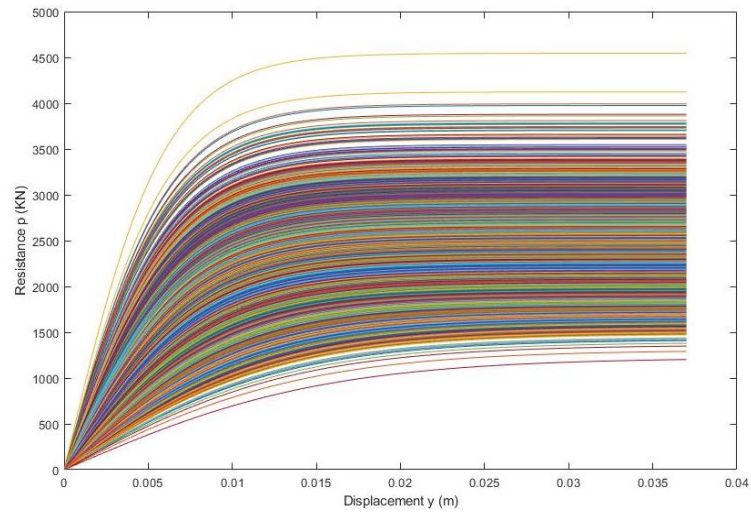


Figure 13 Random p-y curves with the friction angle as random variable

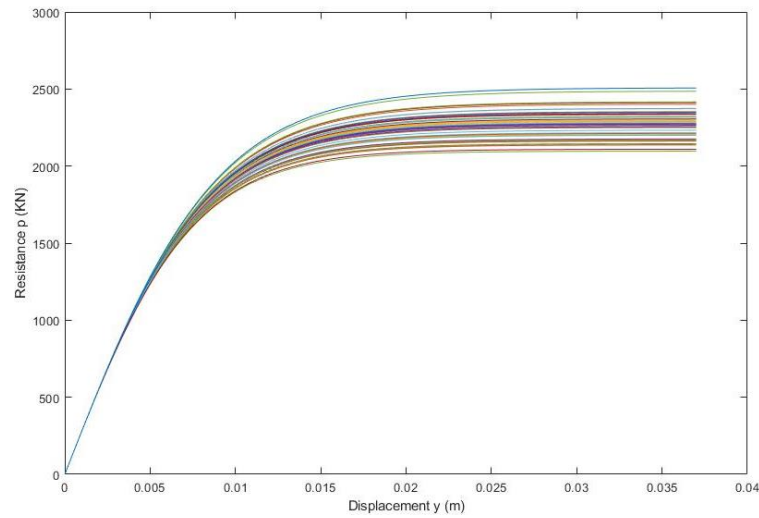


Figure 14 Random p-y curves with the unit weight as random variable

The variability of a random parameter can be defined by the coefficient of variation (CV) which is as follows:

$$CV = \frac{\text{Standard Deviation}}{\text{mean}} \times 100 \quad (14)$$

For sands this coefficient ranges between 5% and 15% (Uzielli, et al., 2006). So herein we will be using a mean of 35 degrees for sands and 41 degrees for the rock dike and the corresponding standard deviation will be set to 3.24 degrees for both layers as shown in Table 3.

Table 3 Mean and Standard Deviation for the soil layers in degrees

| | Mean | Standard Deviation |
|------|------|--------------------|
| Sand | 35° | 3.24° |
| Rock | 41° | 3.24° |

In a random field, all the points must be spatially correlated for a better simulation of reality. Spatial correlation prevents sudden jumps between the values from one point to another but rather allows a smooth transition throughout the field's dimensions. The Markovian correlation is an exponentially decaying spatial correlation structure and widely used in geotechnical problems having a correlation coefficient of:

$$\rho(\tau) = e^{\left(\frac{-2 \times |\tau|}{\theta}\right)} \quad (15)$$

Where τ is the lag distance and θ is the correlation length. Correlation length is the distance within which points are significantly correlated (Fenton and Griffiths, 2008).

But our random field is going to be 2-dimensional where all the springs in the model are correlated to each other vertically and horizontally thus the correlation coefficient becomes:

$$\rho(\tau) = e^{\left(\frac{-2 \times |\tau_x|}{\theta_1}\right)} \cdot e^{\left(\frac{-2 \times |\tau_y|}{\theta_2}\right)} \quad (16)$$

Where τ_x and τ_y are the lag distances in the horizontal and vertical directions respectively, and θ_1 and θ_2 are the horizontal and vertical correlation lengths respectively. The corresponding covariance function will be:

$$C(\tau) = \sigma^2 \cdot \rho(\tau) \quad (17)$$

Where σ is the standard deviation.

The points which constitute the random field are the springs that are distributed along each pile where every spring is correlated vertically and horizontally with the

other springs in the model. A MATLAB code is written to generate random spatially correlated values of friction angle that are then plugged into the p-y relationship thus the p-y curve can be deducted for each random variable and several points that represent this curve are extracted. The process is repeated through 2 loops: the first circulates throughout all the springs in each simulation and the second circulates through all the simulations.

After generating all the random p-y curves for all the simulations, MATLAB will export them to SAP2000 one by one for every simulation in which the model will be analyzed and the required results will be extracted each time. This process is looped through all the simulations in an automated manner.

3.4.MATLAB code

In this section, the structure of the MATLAB code will be discussed thoroughly.

First thing to do is to prepare the correlation matrix and since the only parameters that will vary in that matrix are the vertical and horizontal distances between the springs, X and Y distances matrices are to be constructed. To do this, each one of the 2 matrices is divided into 36 sub-matrices as follows:

First set of sub-matrices: D11, D22,...D66. These are all equal matrices that describe the distance between springs in the same pile. i.e. between each pile's springs and itself (Ex: D11 is distance between all springs in pile 1). And since all spring are spaced equally through every pile then these matrices will be equal in the vertical correlation matrix and null in the horizontal correlation matrix. Note that the number of springs in each pile are assumed to be equal, so we will end up with extra p-y curves that will not be used.

Second set of sub-matrices: D12, D13,...D16, D21, D23,...D26...etc. These matrices describe the horizontal and vertical distances between all springs in one

pile and those in another. For example D12 describes the distances between the springs in and piles 1 and 2. These matrices are symmetrical, so for example D12 will be equal to D21.

150 springs are included in the model, each pile will have 25 springs. So the each distance matrix will be 150 by 150 in size and is constituted of 25 by 25 submatrices. The sub-matrices are ordered as shown in Table 4.

Table 4 The total "Distances Matrix" containing the 36 sub-matrices

| | | | | | |
|-----|-----|-----|-----|-----|-----|
| D11 | D12 | D13 | D14 | D15 | D16 |
| D21 | D22 | D23 | D24 | D25 | D26 |
| D31 | D32 | D33 | D34 | D35 | D36 |
| D41 | D42 | D43 | D44 | D45 | D46 |
| D51 | D52 | D53 | D54 | D55 | D56 |
| D61 | D62 | D63 | D64 | D65 | D66 |

This process is repeated for both directions and the 2 resulted distance matrices are then transformed into correlation matrices by substituting the value of each distance in the Markovian correlation formula presented in equation 16 while using horizontal and vertical correlation lengths of 10 and 1.5 respectively for the preliminary analysis.

The mean and the standard deviation of sand is assigned to all the soil springs then over-ridden by the mean of the rock-dike for the springs that are within 1.5 meter depth.

Since it's not permissible for the p-y formula to allow friction angles of values less than 29 degrees, a lower truncation of the latter value is assigned to the probabilistic distribution. Finally, n random friction angles are sampled from the normal truncated distribution. Figure 15 shows the probability distribution of the sampled

random variables and it's expected to obtain a “bump” on the right side of the histogram as shown due to the friction angle mean in some of the springs being shifted from 35 degrees for the sand layer to 41 degrees for the rock-dike layer. In other words, the latter distribution constitute of the 2 intersecting distributions: The friction angle of the sand layer on the left and the friction angle of the rock-dike layer on the right.

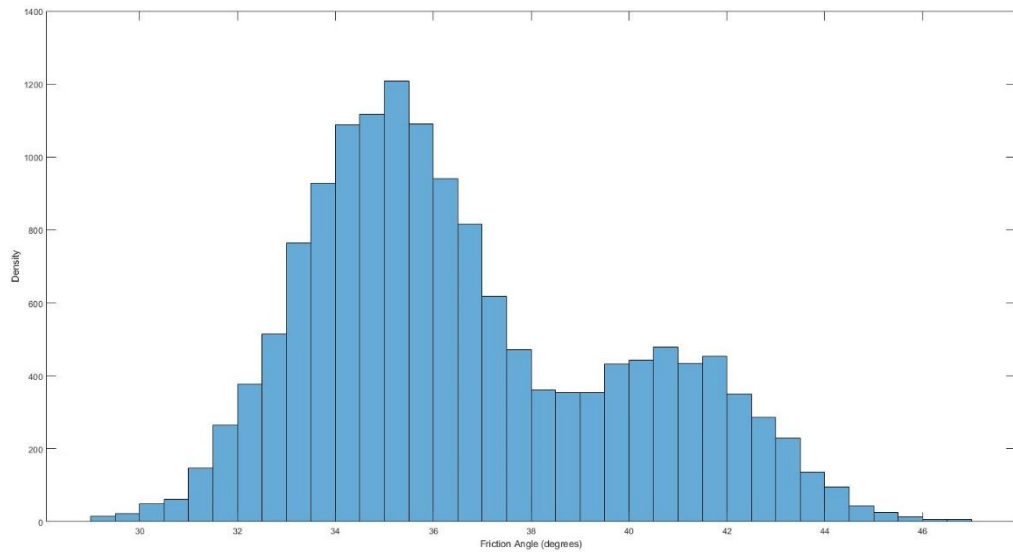


Figure 15 Probability distribution histogram

The random variables are organized in an n by 150 matrix where n being the number of the Monte-Carlo simulations for 150 springs. The structure of the matrix is presented in Table 5.

Table 5 Random variables matrix

| | Spring 1 | Spring 2 | ... | Spring 150 |
|-----------------|-------------|-------------|-----|---------------|
| Simulation 1 | X1,1 | X1,2 | ... | X1,150 |
| Simulation 2 | X2,1 | X2,2 | ... | X2,150 |
| ... | ... | ... | ... | ... |
| Simulation n | Xn,1 | Xn,2 | ... | Xn,150 |

The next step is to transform the variability in the friction angle of the soil into variability in the p-y curves. To do this, the random friction angles are substituted into the p-y formula presented earlier in equation 2 and several points on the p-y curve are extracted for each random variable. The resulted output is a 4-dimensional matrix where its first 2 dimensions being the number of points on the p-y curve and the coordinates p and y, the third dimension is the number of simulations and the fourth dimension is the total number of springs.

Having the random p-y curves generated, MATLAB will then automatically generate “\$.2k” text files (SAP2000 data file format) for the wharf model and copy the p-y curves data for each spring into that file. This process will be repeated for every

simulation, thus generating n “.\$2k” files. The p-y multilinear data assigned to each link/spring within the .\$2k text file is shown in Figure 16.

```

TABLE: "LINK PROPERTY DEFINITIONS 03 - MULTILINEAR"
Link=1.000000 DOF=U1 Fixed=No NonLinear=Yes TransKE=0 TransCE=0 Force=-1.878529 Displ=-0.05
Link=1.000000 DOF=U1 Force=-1.878529 Displ=-0.025
Link=1.000000 DOF=U1 Force=-1.878529 Displ=-0.008
Link=1.000000 DOF=U1 Force=-1.87329 Displ=-0.003
Link=1.000000 DOF=U1 Force=-0.937187 Displ=-0.0005
Link=1.000000 DOF=U1 Force=0 Displ=0
Link=1.000000 DOF=U1 Force=1E-06 Displ=1E-06
Link=1.000000 DOF=U1 Force=0.937187 Displ=0.0005
Link=1.000000 DOF=U1 Force=1.87329 Displ=0.003
Link=1.000000 DOF=U1 Force=1.878529 Displ=0.008
Link=1.000000 DOF=U1 Force=1.878529 Displ=0.025
Link=1.000000 DOF=U1 Force=1.878529 Displ=0.05
Link=10.000000 DOF=U1 Fixed=No NonLinear=Yes TransKE=0 TransCE=0 Force=-73.840821 Displ=-0.05
Link=10.000000 DOF=U1 Force=-73.840821 Displ=-0.025
Link=10.000000 DOF=U1 Force=-73.722092 Displ=-0.008
Link=10.000000 DOF=U1 Force=-64.29323 Displ=-0.003
Link=10.000000 DOF=U1 Force=-16.175064 Displ=-0.0005
Link=10.000000 DOF=U1 Force=0 Displ=0
Link=10.000000 DOF=U1 Force=1E-06 Displ=1E-06
Link=10.000000 DOF=U1 Force=16.175064 Displ=0.0005
Link=10.000000 DOF=U1 Force=64.29323 Displ=0.003
Link=10.000000 DOF=U1 Force=73.722092 Displ=0.008
Link=10.000000 DOF=U1 Force=73.840821 Displ=0.025
Link=10.000000 DOF=U1 Force=73.840821 Displ=0.05
Link=100.000000 DOF=U1 Fixed=No NonLinear=Yes TransKE=0 TransCE=0 Force=-8248.580286 Displ=-0.05
Link=100.000000 DOF=U1 Force=-7831.125373 Displ=-0.025
Link=100.000000 DOF=U1 Force=-4316.541914 Displ=-0.008
Link=100.000000 DOF=U1 Force=-1768.400569 Displ=-0.003
Link=100.000000 DOF=U1 Force=-299.233179 Displ=-0.0005
Link=100.000000 DOF=U1 Force=0 Displ=0
Link=100.000000 DOF=U1 Force=1E-06 Displ=1E-06
Link=100.000000 DOF=U1 Force=299.233179 Displ=0.0005
Link=100.000000 DOF=U1 Force=1768.400569 Displ=0.003
Link=100.000000 DOF=U1 Force=4316.541914 Displ=0.008
Link=100.000000 DOF=U1 Force=7831.125373 Displ=0.025
Link=100.000000 DOF=U1 Force=8248.580286 Displ=0.05

```

Figure 16 p-y multilinear data in .\$2k text file format

Finally, MATLAB will import the .\$2k files into SAP2000 by using operating system commands for example: “C:\SAP2000\SAP2000.EXE” will open SAP2000 then “*file_path*\example.\$2k” will import the .\$2k file “example”; lastly, /R and /C will run the analysis and then close the model respectively. This process is looped over the number of simulations.

SAP2000 has an option to generate an output excel file containing the required results every time the software runs the analysis. So in the previous For loop, MATLAB extracts the following results with each simulation:

- The shear force generated in the first 2 piles at the OLE, CLE and DE limits due to seawards push-over loading.
- The horizontal displacement of the deck at the OLE, CLE and DE limits due to seawards push-over loading.

- The horizontal deck displacement demands due to El-Centro ground motion scaled at $x1g$, $x2g$ and $x3g$ (where g is the gravitational acceleration).

In order to detect the results at certain strain limits, MATLAB records the load step at which each hinge state occurs within every loop and then extract the required results at that corresponding step.

Finally, probabilistic histograms are created representing the outputs of the Monte-Carlo simulations for each type of the results mentioned above.

CHAPTER 4

RESULTS

1. Introduction

In this chapter, the results of the numerical models are presented and analyzed. The chapter is divided into 3 main sections each divided into subsections.

- Deterministic Results
 - Lower Bound Model
 - Upper Bound Model
- Stochastic Results
 - Capacity Probabilistic Distributions
 - Demand Probabilistic Distributions
 - Correlation Length Sensitivity

2. Deterministic Results

2.1. Lower Bound Model Capacity

In the lower bound model, a value of 0.3 is assigned as a p-multiplier for the p-y curves of the associated soils. Figure 17 shows the corresponding push-over curve along with the different limit state points. The base shear reaches to a maximum of 2295 KN with 0.378 m deck horizontal displacement at the design level stage.

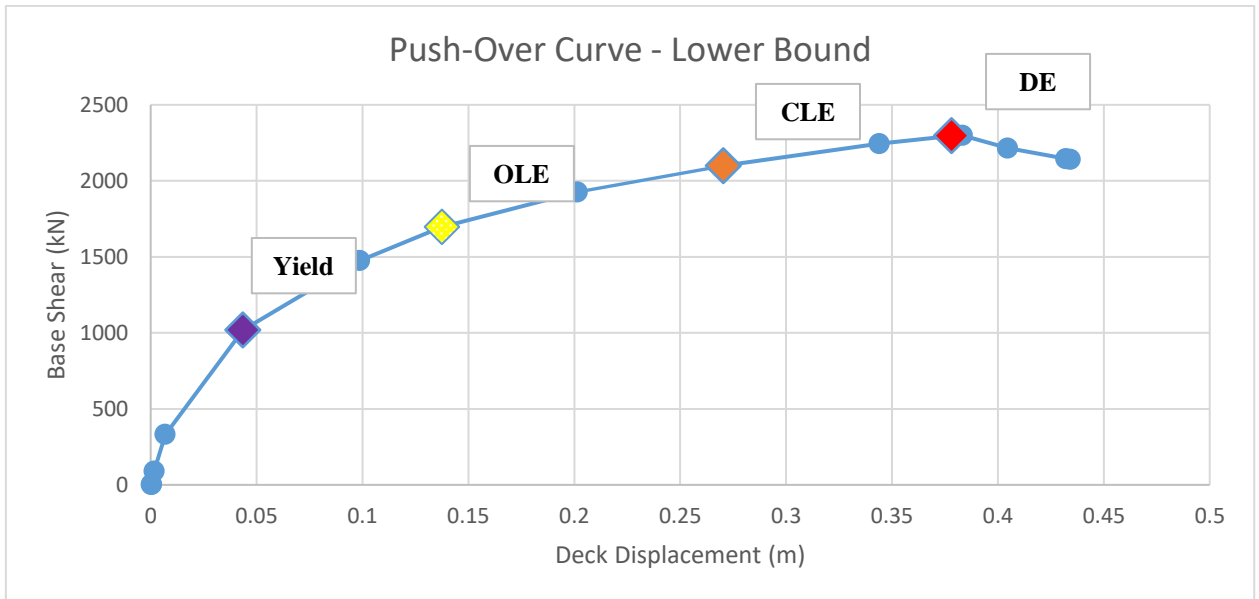


Figure 17 Push-over curve for the lower bound model

Figure 18 shows the sequence of hinge formation for in-ground and top hinges. The first 2 piles are almost always the first to hinge. Having the least free length above the ground level, the latter piles will absorb the most resistance from soil compared to the other piles and thus attract the most stresses which causes them to yield first. As you can see, the pile reached its designated maximum horizontal deck displacement and yet several hinges have not yielded. This is due to the fact that the lower bound soil is more susceptible to deformation due to its lesser resistance which causes the deck to displace faster.

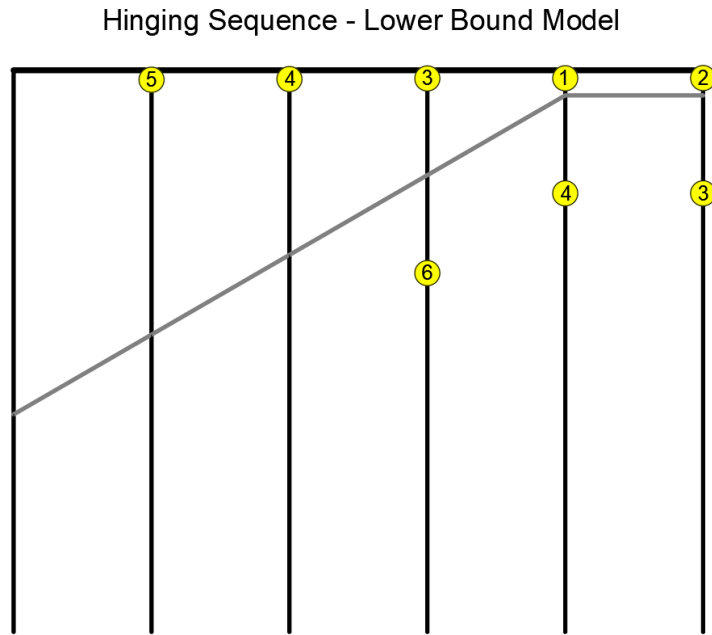


Figure 18 Hinging sequence for the lower bound model

2.2.Upper Bound Model Capacity

In the upper bound model, a value of 2 is assigned as a p-multiplier for the p-y curves of the associated soils. Figure 19 shows the corresponding push-over curve along with the different limit state points. The base shear reaches to a maximum of 3559 KN with 0.235 m deck horizontal displacement at the design level stage.

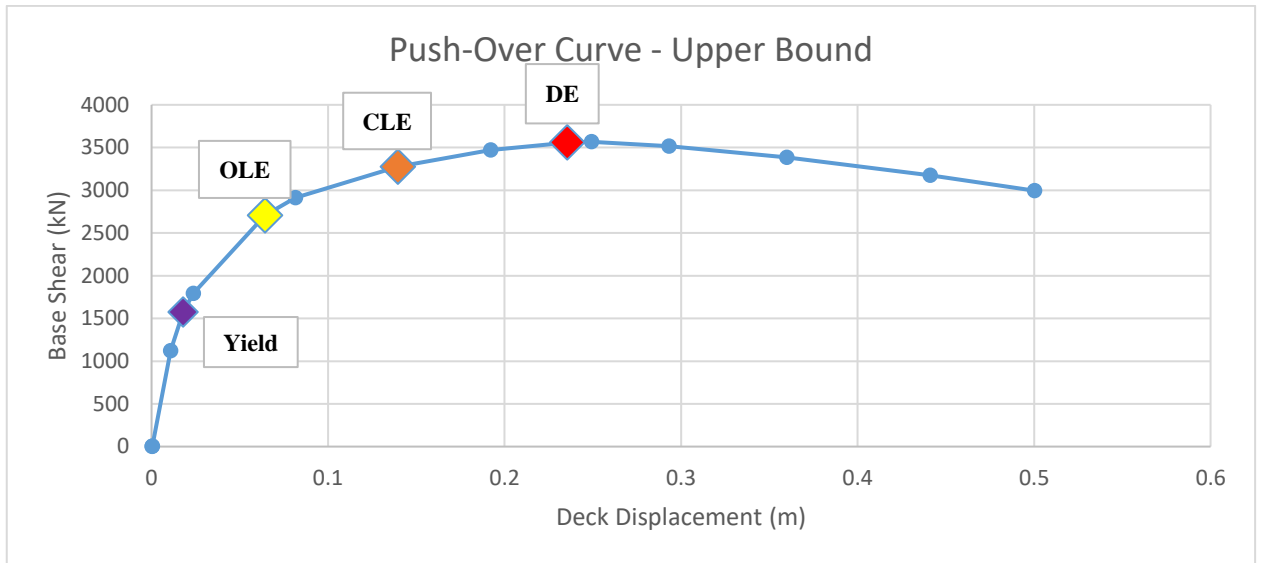


Figure 19 Push-over curve for the upper bound model

Figure 20 shows the sequence of hinge formation for the in-ground and top hinges. Just like the previous model, the first 2 piles are the first to hinge. But on contrary to the lower bound hinging sequence, all hinges were activated when the pile's designated maximum horizontal deck displacement was reached which is due to the higher soil resistance that induce more stresses.

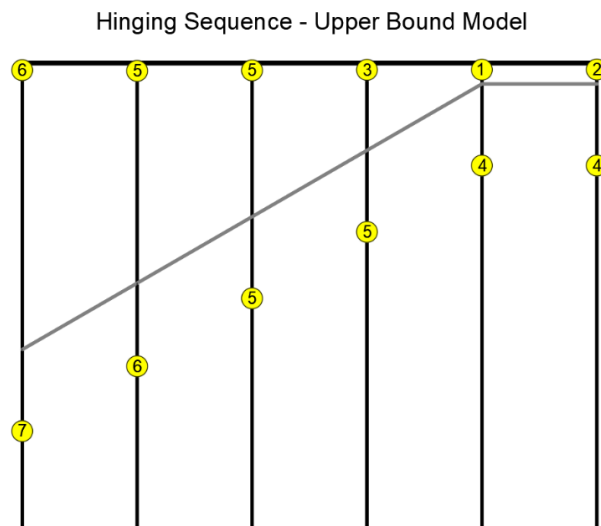


Figure 20 Hinging sequence for the upper bound model

2.3. *Deterministic Demand vs. Capacity*

The wharf structure's upper and lower bounds models are subjected to El-Centro time-history ground motion to be analyzed against the corresponding capacity. In order to capture the structural behavior at different earthquake intensities, the ground motion is scaled at 1g, 2g and 3g where g is the gravitational acceleration on earth (9.81 m/s²). The horizontal deck displacements demand and capacity are presented in Table 6. The demands are obtained by extracting the maximum lateral deck displacement due to the different scales of the El-Centro ground motion while the displacement capacities are recorded at each strain limit when the latter is reached in one or more hinges in the model.

Table 6 Deterministic demand and capacity horizontal deck displacements

| <i>Deterministic Analysis – Horizontal Deck Displacements (m)</i> | | | | | | |
|---|---------------------------|----------------|----------------|-----------------------------|---------------|---------------|
| | Demand (El-Centro) | | | Capacity (Push-over) | | |
| Scales/Limits | 1g | 2g | 3g | OLE | CLE | DE |
| LB Deck Displacement | 0.03771 | 0.09458 | 0.12335 | 0.1376 | 0.2704 | 0.3782 |
| UB Deck Displacement | 0.02689 | 0.07311 | 0.0972 | 0.064 | 0.1396 | 0.2355 |

The failure criteria can be defined as the demand exceeding the capacity. Due to the different free lengths of the piles along the wharf (the length over which the pile is not laterally supported by soil) that affects the lateral stiffness, an eccentricity is formed between the centers of mass and inertia which can result in additional torsional stresses.

To account for the latter torsional effect, the resulted demand displacements are multiplied by a dynamic magnification factor (DMF) as recommended by (Port of Long Beach Wharf Design Criteria, 2015). The DMF depends on the dimensions of the wharf unit and the design levels. For simplicity DMF is set to 1.5.

Table 7 Demand to capacity ratios for the lower bound model

| <i>Lower Bound Model - (Demand/Capacity)*DMF</i> | | | |
|--|---------------|---------------|---------------|
| El-Centro Scale | OLE | CLE | DE |
| x1g | 0.4115 | 0.2094 | 0.1497 |
| x2g | 1.031 | 0.5246 | 0.3751 |
| x3g | 1.345 | 0.6842 | 0.4892 |

Table 7 shows the demand to capacity ratios at different ground motion scales and capacity levels in the lower bound model. The demand exceeds the capacity at OLE limit when the El-Centro ground motion is scaled at both x2g and x3g.

Table 8 Demand to capacity ratios for the upper bound model

| <i>Upper Bound Model - (Demand/Capacity)*DMF</i> | | | |
|--|---------------|---------------|---------------|
| El-Centro Scale | OLE | CLE | DE |
| x1g | 0.6302 | 0.2889 | 0.1713 |
| x2g | 1.7136 | 0.7856 | 0.466 |
| x3g | 2.2783 | 1.0445 | 0.6191 |

Table 8 shows the demand to capacity ratios for the upper bound model. The demand exceeds the capacity at OLE limit for both the x2g and x3g scaled El-Centro and exceeds the CLE limit at x3g only. The above results are summarized in

Figure 21 where the lines in each of the upper and lower bound cases (blue and green) represent the DE, CLE and OLE limits respectively from bottom to top.

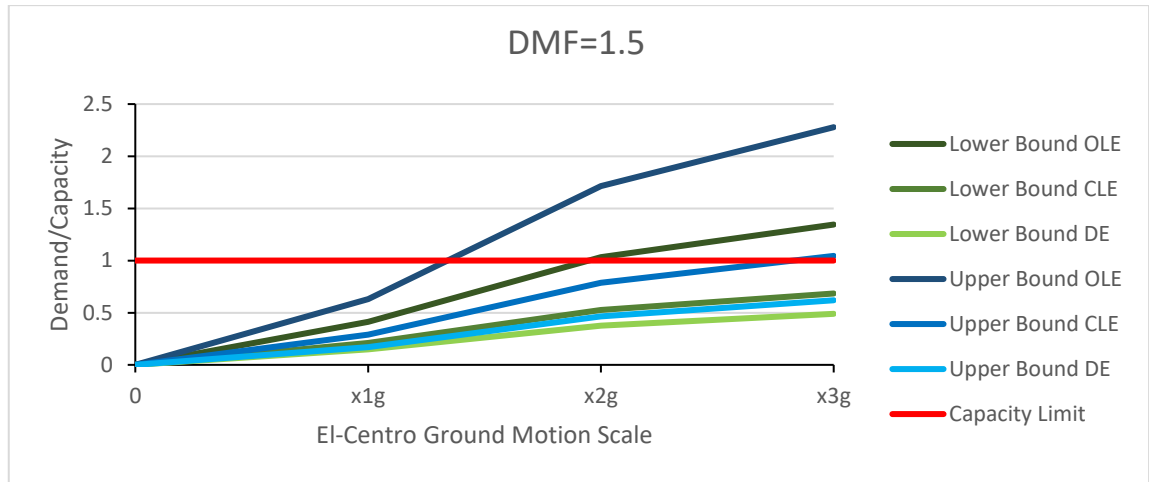


Figure 21 Deterministic Results at DMF=1.5

3. Stochastic Results

The stochastic analysis will generate n numerical simulations of pile supported wharf structures where the soil is defined by springs that exhibits non-linear p-y relationships. The friction angle property of each spring varies within 2-dimensional correlated stochastic fields that are randomly generated with every simulation. After analyzing the latter simulations numerically, the required results are extracted consisting of the push-over analysis displacement and shear capacities on one hand and the displacement demands using El-Centro time history ground motion scaled at x1g, x2g and x3g on the other hand. The preliminary vertical and horizontal correlation lengths in the stochastic analysis are set to 1.5 and 10 respectively. A sensitivity analysis for the correlation length variation is presented later on in this section. The number of simulations generated was 5000 for the push-over analysis and 2000 for the time history ground motion analysis. Those numbers were chosen based on two criteria: The first

being the point at which the shape of the distributions became approximately constant and second being the time constraint when performing the Monte-Carlo simulations.

3.1. Capacity

A displacement based push-over load case is applied on the model where the deck is displaced horizontally to a maximum of 0.5 m while recording the displacements and shear capacities at several time steps. The lateral deck displacement is recorded at OLE, CLE and DE in each simulation. During the push-over analysis, the model is considered to reach a certain hinging limit state when the first hinge in the model has reached that state. Moreover, the maximum generated shear force in the first 2 piles that have the smallest free length is extracted.

Figure 22 shows the probabilistic distribution of the horizontal deck displacement at OLE along with the lower and upper bound deterministic limits at the same level. The generated probabilistic histogram is found to be bi-modal and this is expected due to some variation in the hinging sequence between one simulation and another which causes “jumps” in the lateral deck displacement.

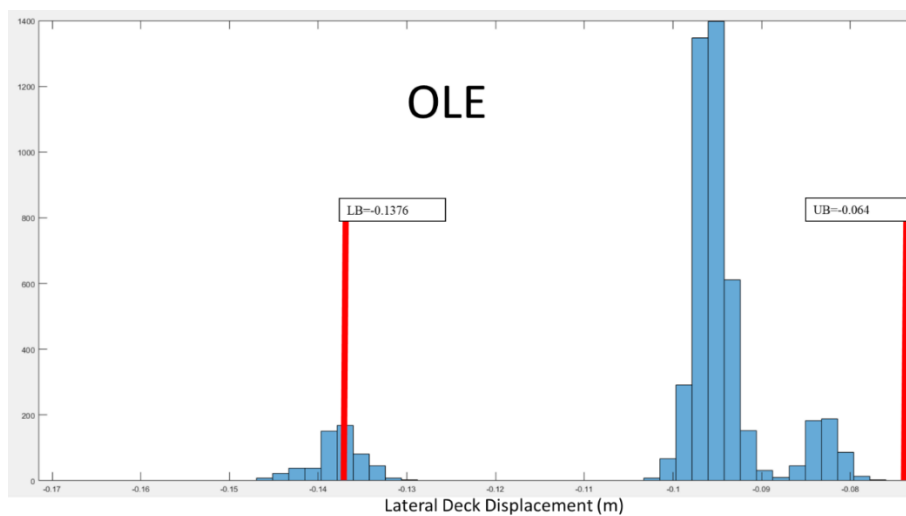


Figure 22 Probabilistic Distribution of Horizontal Deck Displacements at OLE Level

Figure 23 Shows the deformed shape of the wharf model in SAP2000 for 2 distinct simulations having different hinge yielding sequence. In the first simulation, only the first two piles from the right had their in-ground hinge yielded which created a distribution around a displacement of 0.0949 m. While in the second simulation, the third pile from the right has yielded in-ground in addition to the first 2 piles which caused a “jump” in the lateral deck displacement reaching around 0.132 m and this explains the bimodal shape of the distribution.

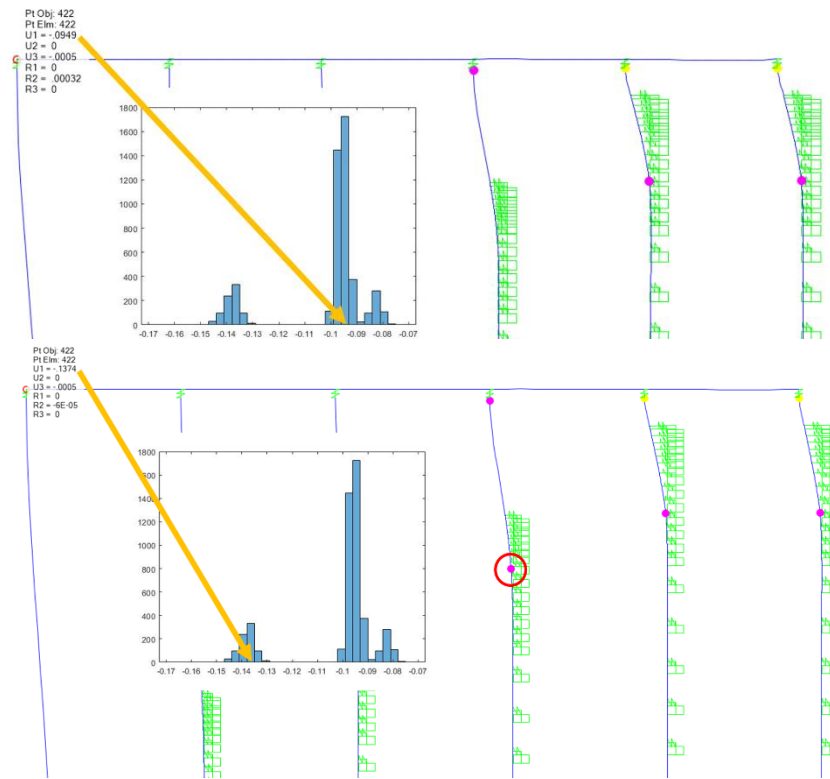


Figure 23 Jumps in the lateral deck displacement due to different hinging sequences

Another Important observation that can be seen in Figure 23 is that a portion of the lateral displacement distribution has exceeded the lower bound limit which raises the questions about how realistic this limit is at the OLE level. About 9.5% of the simulations exceeded the lower bound limit at OLE.

Figure 24 shows the probabilistic distribution of the horizontal deck displacements at CLE. The distribution was bimodal similar to that of the OLE but no exceedance of the lower and upper bounds was detected.

The DE displacements distribution in Figure 25 approaches back to normal. This can be explained by the fact that most plastic hinges are activated at that limit state where the behavior of the random simulations becomes almost uniform as the push-over curve approaches a plateau, preventing sudden “jumps” in the lateral displacements that causes bimodal distributions. Also, the DE distribution was found to be well within the lower and upper bounds range. Only 2×10^{-4} % of the results exceeded the upper bound limit.

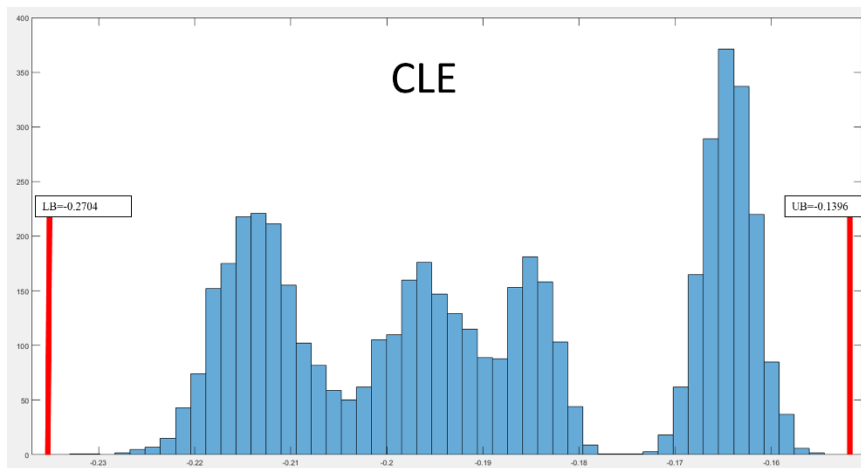


Figure 24 Probabilistic Distribution of Horizontal Deck Displacements at CLE Level

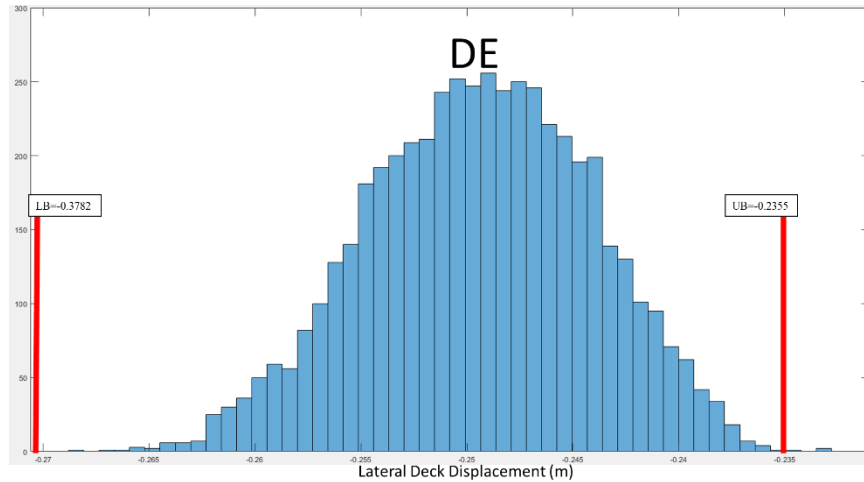


Figure 25 Probabilistic Distribution of Horizontal Deck Displacements at DE Level

Figure 26, Figure 27 and Figure 28 show the maximum shear force distribution in the first 2 piles from the right at OLE, CLE and DE. The resulted distribution was approximately normal as expected since unlike the study of the horizontal deck displacement that is directly dependent on the behavior of all the piles involved, the shear force distribution was extracted from the pile itself and thus eliminating the bimodal effect. It's clear from all the distributions that the results are well within the limits of the upper and lower bounds.

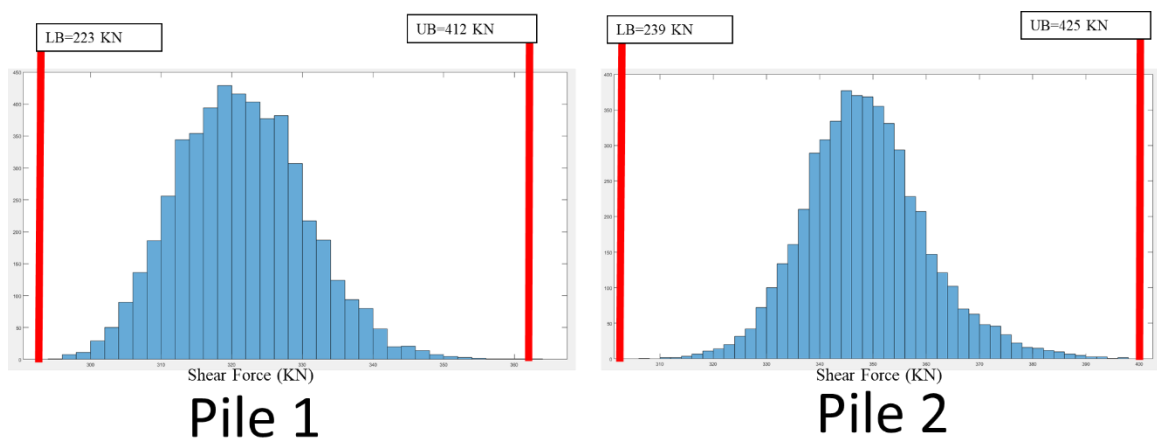


Figure 26 Max shear force distribution in the first 2 piles at OLE

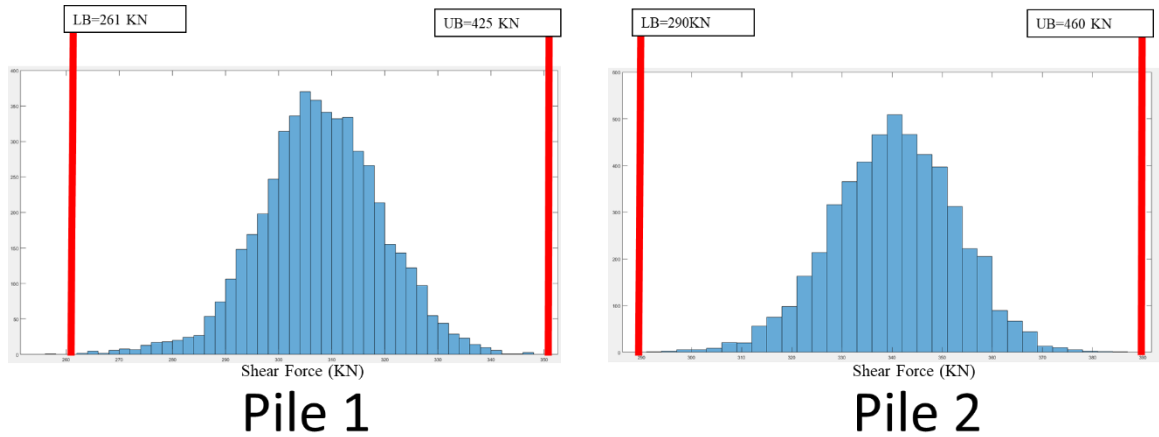


Figure 27 Max shear force distribution in the first 2 piles at CLE

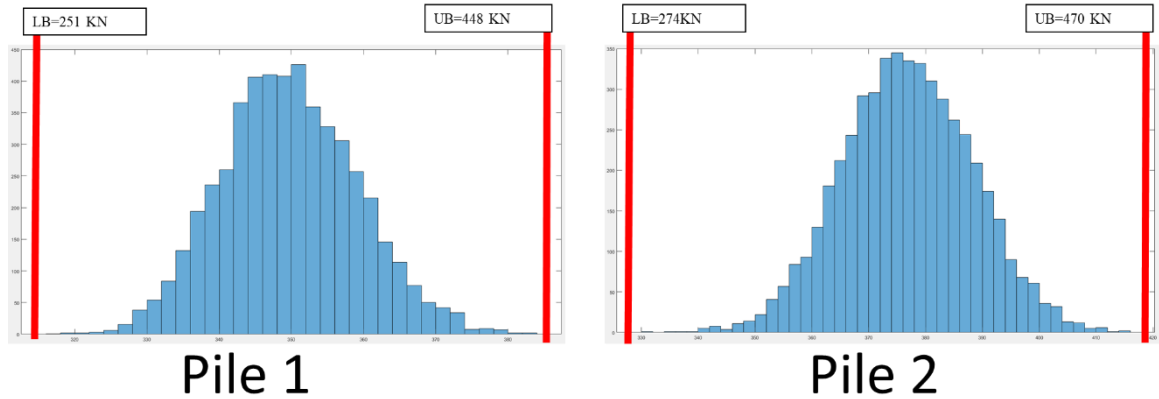


Figure 28 Max shear force distribution in the first 2 piles at DE

3.2.Demand

The demand consists of the El-Centro time history ground motion scaled based on the gravitational acceleration (g) at $x1g$, $x2g$ and $3g$. In order to take into account the additional torsional effect that results from the difference between the centers of mass and rigidity as discussed previously, the demand displacements are multiplied by a dynamic magnification factor equal to 1.5.

The aim is to modify the deterministic performance based analysis by dealing with uncertainties as random variables and thus transforming the outcomes from a

fail/pass ratio into a probability of failure that is influenced by the probability of occurrence of a certain earthquake. Figure 29 shows the maximum horizontal deck displacements distribution due to the scaled El-Centro ground motions. The probability of failure is defined as the probability of obtaining a simulation where maximum horizontal deck displacement due to the different scales of El-Centro ground motion exceeds the same displacement due to push-over analysis at OLE, CLE and DE correspondingly.

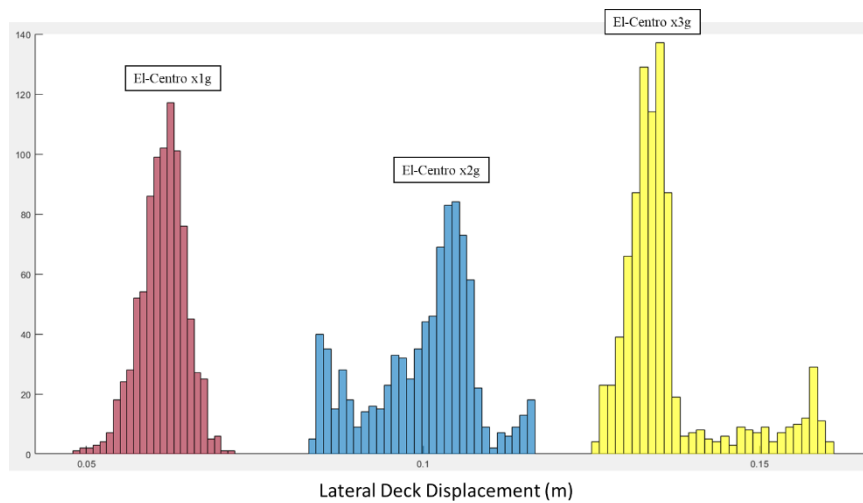


Figure 29 Max El-Centro Horizontal Deck Displacement Demand at x1g, x2g and x3g

Table 9 shows the probability of failure under different ground motion scales and at different design levels. The latter transform the deterministic failure criteria of Table 8 and Table 7 into probabilities of failure that takes into consideration the random variation of the friction angle. Comparing the tables show a compliance between both approaches meaning that when the demand to capacity ratios in the upper and lower bound deterministic models exceeds 1, this will lead to a spike in the probability of failure and vice-versa. Figure 30 clearly presents both approaches.

Table 9 Probability of failure based on 2000 simulation at DMF=1.5

| <i>Probability of Failure - (Failed Simulations/Total Simulations)*100</i> | | | |
|--|---------------|------------|-----------|
| El-Centro Scale | OLE | CLE | DE |
| x1g | 0% | 0% | 0% |
| x2g | 68.05% | 0% | 0% |
| x3g | 92.1% | 0% | 0% |

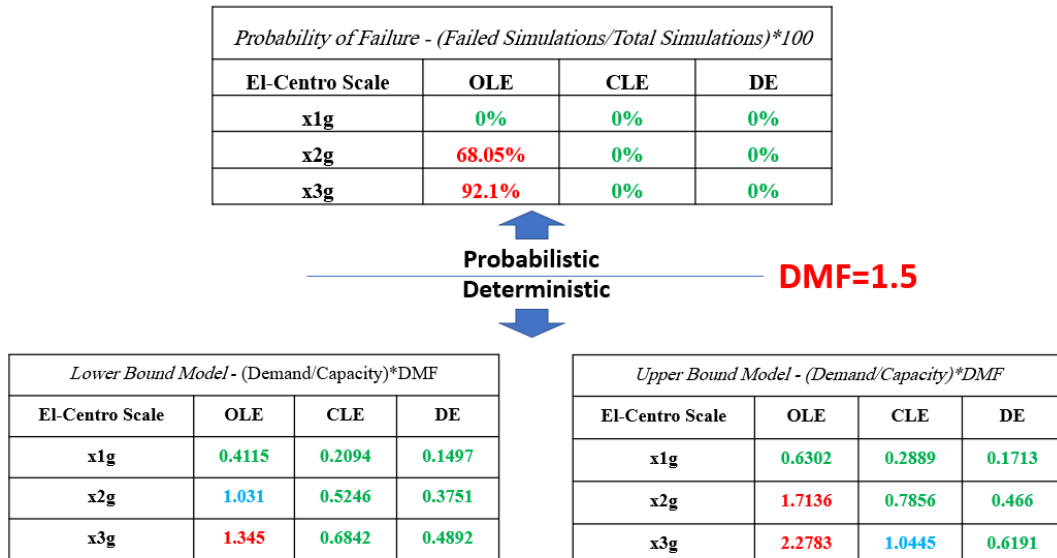


Figure 30 Comparison of deterministic and probabilistic results at DMF=1.5

For the sake of trial, the DMF is increased to 1.9 and the results are presented in Figure 31 and Figure 32. As expected, the probabilities of failure will increase greatly as both, upper and lower bound demands, exceed the allowable limits. In case where the exceedance occur only in one deterministic model such as the exceedance of CLE limit in the upper bound model only due x3g scaled ground motion, the spike in the probability of failure (34.65%) will be milder than the cases where both are exceeded.

It's worth noting that the probabilities will divert from the extremities (0% and

100%) as the number of simulations increases, that's because no mathematical fitting was applicable due to the complicated shape of the distributions and therefore the accuracy of the probabilities rely only on the number of simulations.

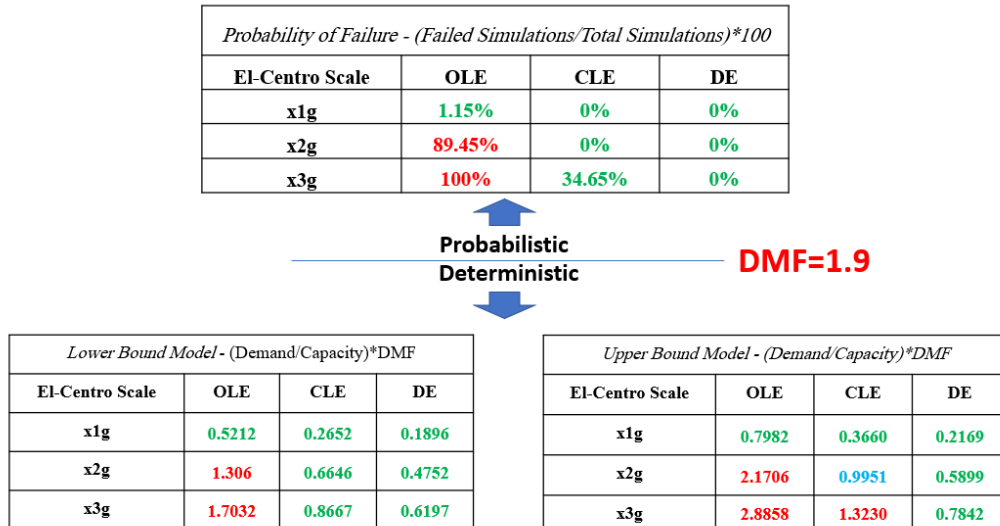


Figure 31 Comparison of deterministic and probabilistic results at DMF=1.9

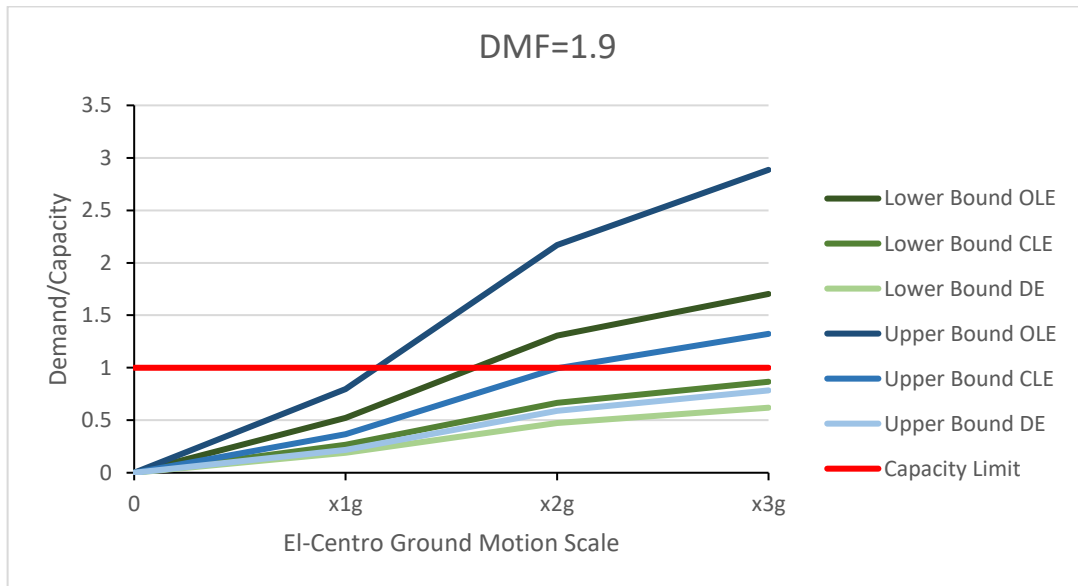


Figure 32 Deterministic Results at DMF=1.9

3.3. Correlation Length Sensitivity

Throughout the 2-dimensional random field, the friction angle of the soil varies gradually from one point to another based on the correlation length. The degree of variation is based on the vertical and horizontal correlation lengths where each spring is correlated in x and y directions with every other spring in the model using the correlation structure presented in chapter 3. Therefore, a sensitivity analysis is important to study the effect of variation of the correlation lengths on the probabilities of failure. The correlations used in x and y directions (θ_x and θ_y respectively) are as follows:

→ $\theta_x=10$, $\theta_y=0.5$.

→ $\theta_x=10$, $\theta_y=1.5$.

→ $\theta_x=10$, $\theta_y=5$.

→ $\theta_x=50$, $\theta_y=1.5$.

→ $\theta_x=100$, $\theta_y=1.5$.

Figure 33 shows the effect of variation of the horizontal correlation length (θ_x) on the probabilistic push-over distributions at various limit states. The distributions fit each other well indicating that the variation in the horizontal correlation has negligible effect on the distributions. This can be explained by the fact that $\theta_x=10$ m will cover almost 2 spans within the wharf model which means that the horizontal points along the first 3 piles, that have considerable effect on the behavior of the wharf model, are well correlated. So a correlation length that is more than 10 meters ($\theta_x=100$ m) will not have an important effect on the structural behavior. It's worth noting that no horizontal correlation length that is less than 10 meters was tested because it's considered to be unrealistic in geotechnical engineering.

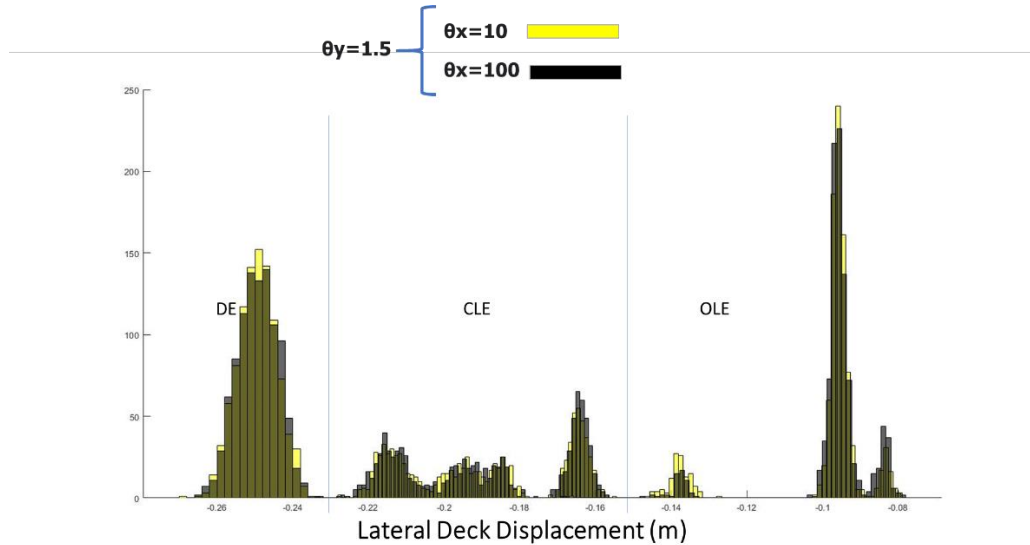


Figure 33 Lateral Deck Displacement at $\theta_x = 10$ and $\theta_x = 100$ for different limit states while θ_y fixed at 1.5

In Figure 34, the effect of vertical correlation length (θ_y) on the lateral deck displacement is studied. When the vertical correlation length increased from 0.5 to 5, the distributions are dispersed indicating an increase in the standard deviation. To quantify this effect, a demand analysis under El-Centro Ground motion scaled at x3g is performed and compared against the OLE push-over capacity limit. The variation of the probability of failure as a function of different vertical correlation lengths is shown in Figure 35 and Figure 36 for the x2g and x3g El-Centro scales respectively. The probability of failure drops from 83.8% to 61.5% for x2g scale and 94.1% to 90.7% for the x3g scale. This proves that the increase in the vertical correlation length for the variation of the friction angle in soils will decrease the probability of failure when dealing with pile supported wharf structures. This phenomenon can be further discussed by observing the effect of the correlation length on behavior of the pile: In high correlation lengths, the variations of the friction angle along the depth of the pile is relatively less dramatic and thus the structural behavior is more uniform and vice versa.

This observation indicates that when there are steeper variations in the friction angle along the depth of the pile, then there's a higher probability that the El-Centro ground motion demand exceeds the push-over capacity in any given simulation. One explanation for this phenomenon is that a higher correlation length means a relatively more uniform soil and thus a more uniform structural behavior which can lead to a relatively lesser amount of generated stresses.

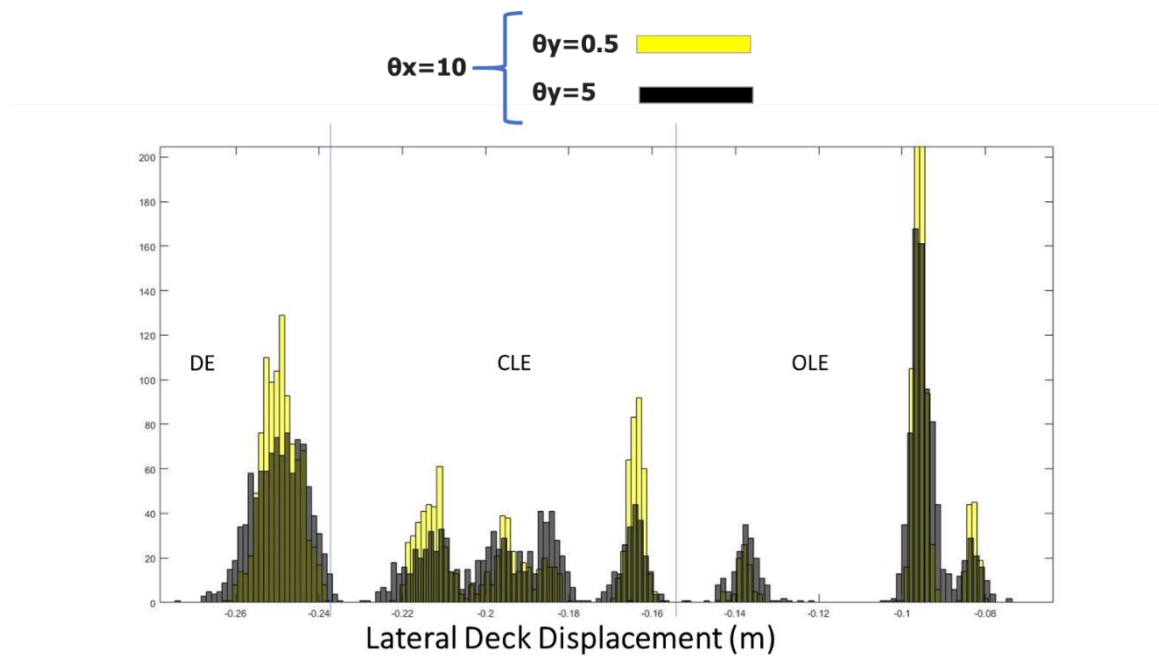


Figure 34 Lateral Deck Displacement at $\theta_y = 0.5$ and $\theta_y = 5$ for different limit states while θ_x fixed at 10

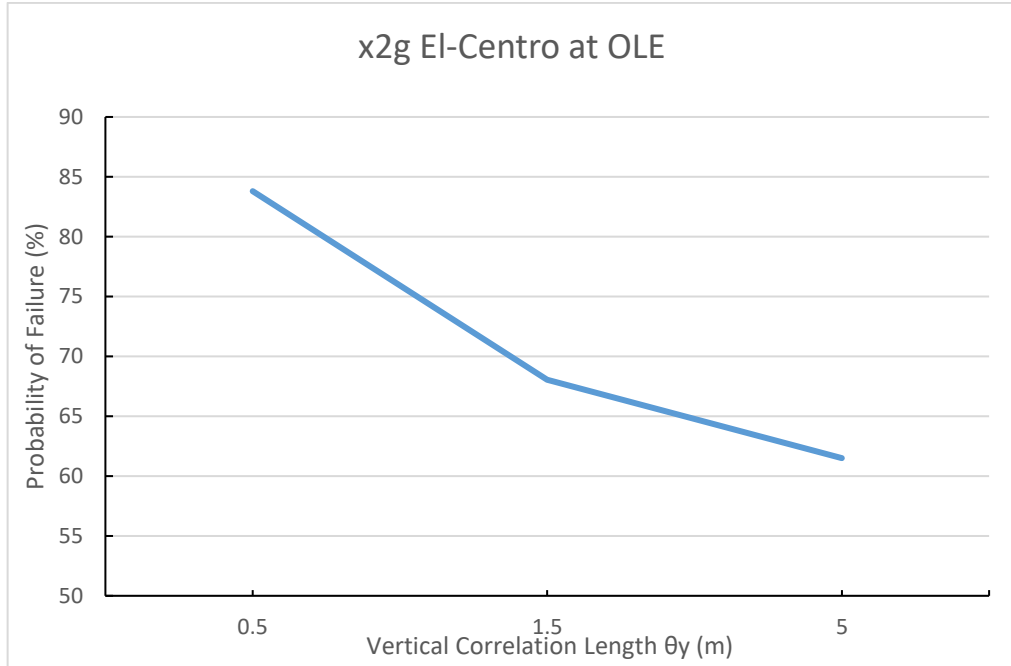


Figure 35 The variation of the probability of failure as a function of the vertical correlation length under x2g El-Centro at OLE limit

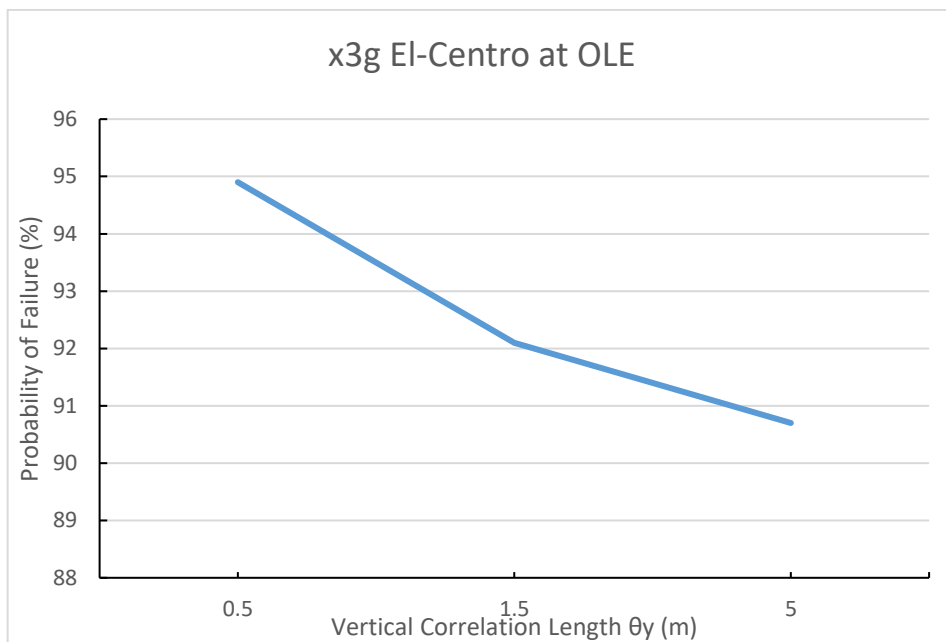


Figure 36 The variation of the probability of failure as a function of the vertical correlation length under x3g El-Centro at OLE limit

CHAPTER 5

CONCLUSION AND RECOMMENDATIONS

1. Conclusion

In this research, the performance of a pile supported wharf structure is studied while taking into consideration the uncertainty of the soil-structure interaction using two distinct approaches: The first is deterministic that imposes upper and lower bounds on the soil resistance and the second is stochastic that treats the mechanical properties of soil (namely the friction angle in sand and rock-dike) as random variables. The performance is assessed by extracting the lateral deck displacement capacities and demands from the latter approaches resulting in deterministic upper and lower bounds values on one side and probabilistic distributions on the other. Finally, the deterministic demand to capacity ratios and the stochastic probabilities of failure are deducted.

The probabilistic results of the lateral deck displacement capacities and demands showed an interesting bi-modal distributions due to the variation of the hinging sequence between various simulations with different friction angle distributions.

Most of the obtained probabilistic distributions are solidified by the code recommendations being tightly fit within the upper and lower bounds range except for the lateral deck displacement at OLE limit where 9.5% of the simulations exceeded the lower bound limit. This raises questions about the reliability of this particular limit against the uncertainty of friction angle in sands.

Moving on to the reliability based design where the deterministic demand to capacity ratios showed a compliance with the stochastic probabilities of failure. When both, the upper and lower bounds demand to capacity ratios exceeds 1 in the

deterministic approach, a relatively high spike in the probability of failure is noticed. On the other hand, when the ratio corresponding to only one of the bounds exceeds the limit, the probability stays relatively low. Since no mathematical fitting was applicable due to the unusual shape of the distributions, the stochastic model is going to need hundreds of thousands of simulations in order to produce highly accurate probabilities that divert from 0% and 100%. This has caused a computational limitation for this research.

The sensitivity of the horizontal and vertical correlation lengths and their effect on the probabilities of failure were also studied. It was shown that the variation of the horizontal correlation length had a negligible effect on the probability of failure because the minimum length of 10 m can already cover the first 2-3 piles that have tremendous effect on the behavior of the wharf so any horizontal correlation length beyond that won't have much impact. On the contrary, the variation of the vertical correlation length affected the probability of failure considerably where the latter probability decreases with the increase of that correlation length. This can be explained the fact that increasing the correlation length will enhance the vertical uniformity of the soil and thus eliminating sudden distortions that cause additional stresses during the soil-structure interaction.

The conclusive points presented in this research are specifically dependent on the conditions that were adopted in the methodology. While some points could be generalized, further research is needed to expand upon this work by testing various uncertainties and structural layouts and come up with ultimate recommendations.

2. Future Work

The work presented herein is to be expanded and improved by further research. Future work suggestions include:

- Studying other sources of geotechnical uncertainties including various soil types such as uncertainties in the cohesion of clays and liquefaction of sands.
- Studying the uncertainties in the seismic demand using fragility curves.
- Performing much higher number of simulations.
- Trying out different structural layouts for the wharf.
- Modeling the soil and its uncertainty as a stochastic finite element continuum.

BIBLIOGRAPHY

- ASCE. (2014). *Seismic Design of Piers and Wharves*. ASCE.
- Chanda, D., Saha, R., & Haldar, S. (2019). Influence of Inherent Soil Variability on Seismic Response of Structure. *Arabian Journal for Science and Engineering*.
- Diaz, G., Patton, B., Armstrong, G., & Joolazadeh, M. (1984). Lateral Test of Piles in Sloping Rock Fill. *Proceeding of ASCE Geotechnical Engineering Division*.
- Esper, P., & Tachibana, E. (1998). *Lessons from the Kobe earthquake*. British Geological / Geotechnical Society.
- European Community of Ship-owners Association. (n.d.). ECSA. Retrieved from www.ecsa.eu
- Fan, H., & Liang, R. (2013). Performance-Based Reliability Analysis of Laterally Loaded Drilled Shafts. *Journal of Geotechnical and Geoenvironmental Engineering*.
- Fenton, & Griffiths. (2008). *Risk Assessment in Geotechnical Engineering*.
- Folke Møller, I., & Christiansen, T. (2011). *Laterally Loaded Monopile in Dry and Saturated Sand*. Masters Dissertation.
- Hamid Heidary-Torkamani, Khosrow Bargi, & Rouhollah Amirabadi. (2013). Seismic vulnerability assessment of pile-supported. *Structure and Infrastructure Engineering*.
- J. McCullough, N., & E. Dickenson, S. (2004). *The Behavior of Piles in Sloping Rock Fill at Marginal Wharves*.
- Kaushik, H. B., & Jain, S. K. (2007). Impact of Great December 26, 2004 Sumatra Earthquake. *JOURNAL OF PERFORMANCE OF CONSTRUCTED FACILITIES* © ASCE.
- Kawamata, Y. (2009). *Full-Scale Lateral Pile Load Test in Rock Fill*. PHD Dissertation.
- Lei Su, W. H.-P., Dong, Y., M. Frangopol, D., & Ling, X.-Z. (2019). Seismic fragility assessment of large-scale pile-supported wharf structures considering soil-pile interaction. *Soil Dynamics and Earthquake Engineering*.
- M. Isenhower, W., & Wang, S.-T. (2013). *Technical Manual for LPILE*. Ensoft.
- Martin, G. (2005). *Port of Los Angeles Seismic Code: Presentation on Geotechnical*. Los Angeles: POLA Seismic Code Workshop.

- Mathukkumaran, Sundaravadivu, & Gandhi. (2008). Effect of Slope on p-y Curves due to Surcharge Load. Soils and Foundations; Japanese geotechnical society.
- Mezazigh, S., & Levacher, D. (1998). Laterally Loaded Piles in Sand: Slope Effect on p-y Reaction Curve. Canadian Geotechnical Journal.
- Mirfattah, & Lai. (2015). Effect of Uncertainties in Soil properties on Probabilistic Seismic Performance of Pile-supported Wharves. 6th International Conference on Earthquake Geotechnical Engineering.
- Mohsen Soltani, & Rouhollah Amirabadi. (2018). Sensitivity Analysis of Pile Supported Wharves against Directional Uncertainty of Earthquakes Using Fragility Curves. INTERNATIONAL JOURNAL OF MARITIME TECHNOLOGY.
- O'Neill, M., & Murchison, J. (1983). An Evaluation of p-y Relationships in Sands. [Houston, Tex.] : University of Houston.
- Port of Long Beach Wharf Design Criteria. (2015). Port of Long Beach (Vol. Version 4.0).
- R. Gregory, M. Harstone, G. J. Rix, M. ASCE, & A. Bostrom. (2012). Seismic Risk Mitigation Decisions at Ports: Multiple Challenges, Multiple Perspectives. ASCE, Natural Hazards Review/ Volume 13 Issue 1.
- Su, L., Wan, H.-P., Dong, Y., M. Frangopol, D., & Ling, X.-Z. (2019). Seismic fragility assessment of large-scale pile-supported wharf structures considering soil-pile interaction. Engineering Structures.
- Talukder, M., & M Lye, L. (2008). Probabilistic Analysis of Laterally Loaded Pile-Soil System using Monte Carlo Simulation. Proceedings of the Eighth (2008) ISOPE Pacific/Asia Offshore Mechanics Symposium.
- Uzielli, M., Farrokh , N., Lacasse, S., & Phoon, K.-K. (2006). Soil Variability Analysis for Geotechnical Practice. Proceedings of the 2nd International Workshop on Characterisation and Engineering Properties of Natural Soil.
- Vermeer, P. A., Bardossy, A., & Hicks, M. A. (2013). Soil variability and its consequences. Institut für Geotechnik der Universität Stuttgart.
- worldview.stratfor.com. (2012).

APPENDIX

MATLAB Code

```
%*****INPUTS*****

S=SpringsConfiguration{:,:}; %Depth of each spring/distance from *1st Spring*
in meters
R=[0 5.5 11 16.5 22 27.5]; %horizontal location of each pile
T=TributaryWidths{:,:}; %Tributary width for each spring

Dia=0.65; %Diameter of the pile in meters
U=16; %Unit weight of Sand in Kn/m3
U_rock=21; %Unit weight of rock fill in Kn/m3
avg=35; %Mean of the Friction Angle of Sand
Layer
avg_rock=41; %Mean of thr Friction Angle of Rock
Dike Layer
sigma=3.24; %Standard Deviation of the Friction
Angle of Sand and Rock Dike layers
theta=30; %Slope angle of the ground
CLx=10; %Correlation Length
CLy=5;
Simulations=2000; %Number of simulations

%*****END OF INPUTS*****

n=size(S,1);

%x-direction matrix

D11x=zeros(25,25);
D22x=zeros(25,25);
D33x=zeros(25,25);
D44x=zeros(25,25);
D55x=zeros(25,25);
D66x=zeros(25,25);

D12x=5.5*ones(25,25);
D13x=11*ones(25,25);
D14x=16.5*ones(25,25);
D15x=22*ones(25,25);
D16x=27.5*ones(25,25);

D23x=5.5*ones(25,25);
D24x=11*ones(25,25);
D25x=16.5*ones(25,25);
D26x=22*ones(25,25);

D34x=5.5*ones(25,25);
D35x=11*ones(25,25);
D36x=16.5*ones(25,25);

D45x=5.5*ones(25,25);
D46x=11*ones(25,25);

D56x=5.5*ones(25,25);
```

```

D21x=D12x.';
D31x=D13x.';
D32x=D23x.';
D41x=D14x.';
D42x=D24x.';
D43x=D34x.';
D51x=D15x.';
D52x=D25x.';
D53x=D35x.';
D54x=D45x.';
D61x=D16x.';
D62x=D26x.';
D63x=D36x.';
D64x=D46x.';
D65x=D56x.';

Dx=[D11x D12x D13x D14x D15x D16x;
     D21x D22x D23x D24x D25x D26x;
     D31x D32x D33x D34x D35x D36x;
     D41x D42x D43x D44x D45x D46x;
     D51x D52x D53x D54x D55x D56x;
     D61x D62x D63x D64x D65x D66x];

%y-direction matrix

for i=1:n
    for j=1:n
        D11y(i,j)=abs(S(i,1)-S(j,1));
        D22y(i,j)=abs(S(i,2)-S(j,2));
        D33y(i,j)=abs(S(i,3)-S(j,3));
        D44y(i,j)=abs(S(i,4)-S(j,4));
        D55y(i,j)=abs(S(i,5)-S(j,5));
        D66y(i,j)=abs(S(i,6)-S(j,6));

        D12y(i,j)=abs(S(i,1)-S(j,2));
        D13y(i,j)=abs(S(i,1)-S(j,3));
        D14y(i,j)=abs(S(i,1)-S(j,4));
        D15y(i,j)=abs(S(i,1)-S(j,5));
        D16y(i,j)=abs(S(i,1)-S(j,6));

        D23y(i,j)=abs(S(i,2)-S(j,3));
        D24y(i,j)=abs(S(i,2)-S(j,4));
        D25y(i,j)=abs(S(i,2)-S(j,5));
        D26y(i,j)=abs(S(i,2)-S(j,6));

        D34y(i,j)=abs(S(i,3)-S(j,4));
        D35y(i,j)=abs(S(i,3)-S(j,5));
        D36y(i,j)=abs(S(i,3)-S(j,6));

        D45y(i,j)=abs(S(i,4)-S(j,5));
        D46y(i,j)=abs(S(i,4)-S(j,6));

        D56y(i,j)=abs(S(i,5)-S(j,6));

    end
end

D21y=D12y.';
D31y=D13y.';
D32y=D23y.';
D41y=D14y.';
D42y=D24y.';
D43y=D34y.';
D51y=D15y.';
D52y=D25y.';
D53y=D35y.';

```

```

D54y=D45y.';
D61y=D16y.';
D62y=D26y.';
D63y=D36y.';
D64y=D46y.';
D65y=D56y.';

Dy=[D11y D12y D13y D14y D15y D16y;
     D21y D22y D23y D24y D25y D26y;
     D31y D32y D33y D34y D35y D36y;
     D41y D42y D43y D44y D45y D46y;
     D51y D52y D53y D54y D55y D56y;
     D61y D62y D63y D64y D65y D66y];

o=size(Dx,1); %number of springs
CorrMat=zeros(size(Dx,1),size(Dy,2));
for ie=1:o
    for je=1:o

        CorrMat(ie,je)=exp((-2*Dx(ie,je))/CLx+((-2*Dy(ie,je))/CLy));

    end
end

m_log=log((avg^2)/sqrt(sigma^2+avg^2));
s_log=sqrt(log(sigma^2/(avg^2)+1));

%Generating mean and standard deviation matrices
Mu=zeros(1,o);
Sigma=zeros(1,o);

for e=1:o

    Mu(1,e)=avg;
    Sigma(1,e)=sigma;

end

%Adjusting the mean array to add rock dike layer of thickness 1.5 m

Mu(1:7)=avg_rock;
Mu(26:32)=avg_rock;
Mu(51:57)=avg_rock;
Mu(76:82)=avg_rock;
Mu(101:107)=avg_rock;
Mu(126:132)=avg_rock;

mu      = Mu;
sigMat  = sigma*CorrMat;
NUM_smp=Simulations;
lb=ones(1,o)*29;
ub=ones(1,o)*99;
%Multivariate Truncated Normal Sampling
smpOut  = nan(NUM_smp,numel(lb));
NUM_try = NUM_smp; % trial size
NUM_cur = 0;      % current accepted number
while NUM_cur<NUM_smp
    tmpSmp = mvnrnd(mu, sigMat, NUM_try); % sample MVN
    indAcc = all(tmpSmp > repmat(lb, [NUM_try 1]), 2) & ... % check if
within LB and UB
    all(tmpSmp < repmat(ub, [NUM_try 1]), 2);
    numAcc = sum(indAcc);
    if(numAcc) % record accepted samples
        iS = NUM_cur+1;
    end
end

```



```

        iE = iS + numAcc - 1;
        if(iE>NUM_smp)
            iE = NUM_smp;
            indAcc = find(indAcc);
            indAcc = indAcc(1:(iE-iS+1));
        end
        smpOut(iS:iE,:) = tmpSmp(indAcc,:);
    end
    NUM_cur = NUM_cur + numAcc; % increment
counter
    NUM_try = round((NUM_smp-numAcc) * NUM_try/numAcc); % estimate next
trial size
    NUM_try = min(NUM_try,10*NUM_smp); % limit max trial
size
end

histogram(smpOut)
phi_rnd=smpOut;

s=size(phi_rnd,1); %Number of random variables in each spring

%defining 4D matrix for springs as follows: spring=cell(no of pts on curve, x
and y, number of simulations, number of springs)

spring=zeros(6,2,Simulations,o);

Depth=[S(:,6); S(:,6); S(:,6); S(:,6); S(:,6); S(:,6)]; %transforimng depths
into a column matrix

for j=1:o
    z=Depth(j,1)+0.12; %****YOU NEED TO ADD THE DISTANCE FROM THE FIRST
SPRING TO THE GROUND SURFACE! //or u don't//****

    %Assigning proper unit weight for the rock dike layer
    if any(1:7==j)==1 | any(26:32==j)==1 | any(51:57==j)==1 | any(76:82==j)==1
| any(101:107==j)==1 | any(126:132==j)==1
        U_1=U_rock;
    else
        U_1=U;
    end

    for i=1:s
        phi=phi_rnd(i,j);

        A=3-(0.8*z)/Dia;

        if A<0.9
            A=0.9;
        end

        k=0.00829*phi^4.384-12710;
        a=phi/2;
        b=45+phi/2;
        %Ko is the lateral earth pressure at rest taken 0.4

        %Coefficients for the P ultimate

```

```

D1=(tand(b)*tand(theta))/(tand(b)*tand(theta)+1);
D2=1-D1;
D3=(tand(b)*tand(theta))/(1-tand(b)*tand(theta));
D4=1+D3;
ka=cosd(theta)*((cosd(theta)-sqrt(abs((cosd(theta))^2-
(cosd(phi))^2)))/((cosd(theta)+sqrt(abs((cosd(theta))^2-
(cosd(phi))^2)))));

%Infront of pile:
Pu1=U_1*z*((0.4*z*tand(phi)*sind(b)*(4*D1^3-3*D1^2+1))/(tand(b-
phi)*cosd(a))+(tand(b)*(Dia*D2+z*tand(b)*tand(a)*D2^2)/tand(b-
phi)+0.4*z*tand(b)*(tand(phi)*sind(b)-tand(a))*(4*D1^3-3*D1^2+1)-ka*Dia);

Pu=Pu1;

if Pu==0
    pu=0.00001;
end

yx=(0:0.001:0.07);

%p-y Relationship
syms yx;
p(yx)=A*Pu*tanh((k*z*yx)/(A*Pu));

p1=double(p(0.0005))*T(j,1);
p2=double(p(0.003))*T(j,1);
p3=double(p(0.008))*T(j,1);
p4=double(p(0.025))*T(j,1);
p5=double(p(0.05))*T(j,1);

spring(:, :, i, j)=[0 0; 0.0005 p1; 0.003 p2; 0.008 p3; 0.025 p4;
0.05 p5];

end
end

%%%%%%%%%%%%%%%%%%%%%%%%%%%%%%%%%%%%%%%%%%%%%%%%%%%%%%%%%%%%%%%%%%%%%%%%%PY CURVES ARE GENERATED %%%%%%%%%%%%%%%%%%%%%%%%%%%%%%%%%%%%%%%%%%%%%%%%%%%%%%%%%%%%%%%%%%%%%%%%%%

%P-y tables for positive side
v=1;
for p=1:Simulations
    c=1;
    for u=1:o

        Sx(c:c+5, [v v+1])=flipud(spring(:, :, p, u));
        c=c+6;

    end
    v=v+2;
end

%Replacing zeroes with a small number
Sx(Sx==0)=0.000001;

```

```

%P-y tables for negative side
v=1;
for p=1:Simulations
    c=1;
    for u=1:o

        Sx2(c:c+5,[v v+1])=-spring(:, :,p,u);
        c=c+6;

    end
    v=v+2;
end

%Joining negative and positive parts
v=1;
for p=1:Simulations
    c=1;
    k=1;
    for u=1:o
        Sxf(k:k+11,[v v+1])=flipud([Sx(c:c+5,[v v+1]);Sx2(c:c+5,[v v+1])]);
        c=c+6;
        k=k+12;
    end
    v=v+2;
end
%Removing nan values
Sxf(isnan(Sxf))=0;

%Writing the output according to SAP2000 S2K format
LINK={'Link='};
Space={};
DOF={' DOF=U1'};
DOF2={' DOF=U1 Fixed=No NonLinear=Yes TransKE=0 TransCE=0'};
FORCE={' Force='};
DISPL={' Displ='};
LinkMat=repelem((1:o)',12,1); %This line depends on NUMBER of Points on PY
curves and the TOTAL NUMBER of SPRINGS!
c=1;
q=1:12:7080; %q is used for repeating the first line of the s2k table

for z1=1:Simulations
    for z2=1:size(Sxf,1)
        if ismember(z2,q)==1

            Output_0{z2,1}=LINK;
            Output_0{z2,2}=LinkMat(z2,1);
            Output_0{z2,3}=DOF2;
            Output_0{z2,4}=FORCE;
            Output_0{z2,5}=Sxf(z2,c+1);
            Output_0{z2,6}=DISPL;
            Output_0{z2,7}=Sxf(z2,c);

        else

            Output_0{z2,1}=LINK;
            Output_0{z2,2}=LinkMat(z2,1);
            Output_0{z2,3}=DOF;
            Output_0{z2,4}=FORCE;
            Output_0{z2,5}=Sxf(z2,c+1);
            Output_0{z2,6}=DISPL;
            Output_0{z2,7}=Sxf(z2,c);
        end
    end
end

```

```

        end

        Output{z1}=Output_0;

    end
    c=c+2;
end

%Generating copies of the $2k file template and renamed as Output_n
for k=1:Simulations
    filename=sprintf('Output_%d.$2k',k);
    copyfile ('Original.$2k',filename)
end

%Generating n Output $2k files

for i=1:Simulations

    MyCell=Output{1,i};
    [maxrow, maxcolumn]=size(MyCell);
    FileName=sprintf('Output_%d.$2k',i);
    id = fopen(FileName,'a+t');
    if id<0
        error('could not open file');
    end
    for ro =1:maxrow
        for co =1:maxcolumn
            data=MyCell{ro,co};
            if isa(data,'cell')
                %assume a nested cell with a char array
                fprintf(id,'%10s',data{1});
            else
                %assume a numeric type
                fprintf(id,'%0.6f',data);
            end
        end
        fprintf(id,'\n');
    end
    fclose(id);
end

%Running SAP2000 from windows command prompt and then saving the horizontal
displacement at node
%Results=(no of steps, 3:Step no; Disp at joint 422; Hinge status,
Simulations)

disp_OLE=zeros(1,Simulations);
disp_CLE=zeros(1,Simulations);
disp_DE=zeros(1,Simulations);

M_max_pos=zeros(Simulations,1);
M_max_neg=zeros(Simulations,1);
V_max_pos=zeros(Simulations,1);
V_max_neg=zeros(Simulations,1);
%d_max=zeros(Simulations,1);
Results_Hinges=zeros(14,3,Simulations);

for v=1:366
    %command=sprintf('C:\\Program Files\\Computers and Structures\\SAP2000
19\\SAP2000.EXE" "G:\\Thesis Main\\modeling\\The Final Code\\Output_%d.$2k"
/R /C',v);

```

```

command=sprintf('G:\SAP2000\SAP2000.EXE" "G:\Thesis
Main\modeling\The Final Code\Output_%d.$2k" /R /C',v);
dos(command)
FileName=sprintf('Results_%d.xls',v);
copyfile ('Results.xls',FileName)

%Reading xls output file
[F,F_txt,F_raw]=xlsread('Results.xls','Element Forces - Frames');
[numT,textT,rowT]=xlsread('Results.xls','Joint Displacements');
[num,text,row]=xlsread('Results.xls','Frame Hinge States');

%removing 1st 3 useless rows from text matrix
text(1,:)=[];
text(1,:)=[];
text(1,:)=[];

%"for" loop for identifying hinges
clear H1; clear H2; clear H3; clear H4; clear H5; clear H6; clear H7;
clear H8; clear H9; clear H10; clear H11; clear H12;
for i=1:size(num,1)

    if strcmp(text(i,7),'10H1')==1

        %%%%%%%%%%%%%%%
        if strcmp(text(i,22),'A to B')==1
            H1(i,1)=1;
        elseif strcmp(text(i,22),'B to C')==1
            H1(i,1)=2;
        elseif strcmp(text(i,22),'C to D')==1
            H1(i,1)=3;
        elseif strcmp(text(i,22),'D to E')==1
            H1(i,1)=4;
        elseif strcmp(text(i,22),'>E')==1
            H1(i,1)=5;
        else
            disp('Error')
        end

        %%%%%%%%%%%%%%%
    elseif strcmp(text(i,7),'26H1')==1

        %%%%%%%%%%%%%%%
        if strcmp(text(i,22),'A to B')==1
            H2(i,1)=1;
        elseif strcmp(text(i,22),'B to C')==1
            H2(i,1)=2;
        elseif strcmp(text(i,22),'C to D')==1
            H2(i,1)=3;
        elseif strcmp(text(i,22),'D to E')==1
            H2(i,1)=4;
        elseif strcmp(text(i,22),'>E')==1
            H2(i,1)=5;
        else
            disp('Error')
        end

        %%%%%%%%%%%%%%%
    elseif strcmp(text(i,7),'27H1')==1

        %%%%%%%%%%%%%%%
        if strcmp(text(i,22),'A to B')==1
            H3(i,1)=1;
        elseif strcmp(text(i,22),'B to C')==1
            H3(i,1)=2;
        elseif strcmp(text(i,22),'C to D')==1

```

```

        H3(i,1)=3;
    elseif strcmp(text(i,22),'D to E')==1
        H3(i,1)=4;
    elseif strcmp(text(i,22),'>E')==1
        H3(i,1)=5;
    else
        disp('Error')
    end

    %%%%%%%%%%%%%%
elseif strcmp(text(i,7),'28H1')==1

    %%%%%%%%%%%%%%
    if strcmp(text(i,22),'A to B')==1
        H4(i,1)=1;
    elseif strcmp(text(i,22),'B to C')==1
        H4(i,1)=2;
    elseif strcmp(text(i,22),'C to D')==1
        H4(i,1)=3;
    elseif strcmp(text(i,22),'D to E')==1
        H4(i,1)=4;
    elseif strcmp(text(i,22),'>E')==1
        H4(i,1)=5;
    else
        disp('Error')
    end

    %%%%%%%%%%%%%%
elseif strcmp(text(i,7),'29H1')==1

    %%%%%%%%%%%%%%
    if strcmp(text(i,22),'A to B')==1
        H5(i,1)=1;
    elseif strcmp(text(i,22),'B to C')==1
        H5(i,1)=2;
    elseif strcmp(text(i,22),'C to D')==1
        H5(i,1)=3;
    elseif strcmp(text(i,22),'D to E')==1
        H5(i,1)=4;
    elseif strcmp(text(i,22),'>E')==1
        H5(i,1)=5;
    else
        disp('Error')
    end

    %%%%%%%%%%%%%%
elseif strcmp(text(i,7),'30H1')==1

    %%%%%%%%%%%%%%
    if strcmp(text(i,22),'A to B')==1
        H6(i,1)=1;
    elseif strcmp(text(i,22),'B to C')==1
        H6(i,1)=2;
    elseif strcmp(text(i,22),'C to D')==1
        H6(i,1)=3;
    elseif strcmp(text(i,22),'D to E')==1
        H6(i,1)=4;
    elseif strcmp(text(i,22),'>E')==1
        H6(i,1)=5;
    else
        disp('Error')
    end

    %%%%%%%%%%%%%%
elseif strcmp(text(i,7),'150H1')==1

```

```

%%%%%%%%%%%%%%%%%%%%%%%%%%%%%%%%%%%%%%%%%%%%%%%%%%%%%%%%%%%%%%%%%%%%%%%%
if strcmp(text(i,22),'A to B')==1
    H7(i,1)=1;
elseif strcmp(text(i,22),'B to C')==1
    H7(i,1)=2;
elseif strcmp(text(i,22),'C to D')==1
    H7(i,1)=3;
elseif strcmp(text(i,22),'D to E')==1
    H7(i,1)=4;
elseif strcmp(text(i,22),'>E')==1
    H7(i,1)=5;
else
    disp('Error')
end

%%%%%%%%%%%%%%%%%%%%%%%%%%%%%%%%%%%%%%%%%%%%%%%%%%%%%%%%%%%%%%%%%%%%%%%%
elseif strcmp(text(i,7),'170H1')==1

    %%%%%%%%%%%%%%%%%%%%%%%%%%%%%%%%%%%%%%%%%%%%%%%%%%%%%%%%%%%%%%%%%%%%%%%%%
    if strcmp(text(i,22),'A to B')==1
        H8(i,1)=1;
    elseif strcmp(text(i,22),'B to C')==1
        H8(i,1)=2;
    elseif strcmp(text(i,22),'C to D')==1
        H8(i,1)=3;
    elseif strcmp(text(i,22),'D to E')==1
        H8(i,1)=4;
    elseif strcmp(text(i,22),'>E')==1
        H8(i,1)=5;
    else
        disp('Error')
    end

    %%%%%%%%%%%%%%%%%%%%%%%%%%%%%%%%%%%%%%%%%%%%%%%%%%%%%%%%%%%%%%%%%%%%%%%%%
elseif strcmp(text(i,7),'193H1')==1

    %%%%%%%%%%%%%%%%%%%%%%%%%%%%%%%%%%%%%%%%%%%%%%%%%%%%%%%%%%%%%%%%%%%%%%%%%
    if strcmp(text(i,22),'A to B')==1
        H9(i,1)=1;
    elseif strcmp(text(i,22),'B to C')==1
        H9(i,1)=2;
    elseif strcmp(text(i,22),'C to D')==1
        H9(i,1)=3;
    elseif strcmp(text(i,22),'D to E')==1
        H9(i,1)=4;
    elseif strcmp(text(i,22),'>E')==1
        H9(i,1)=5;
    else
        disp('Error')
    end

    %%%%%%%%%%%%%%%%%%%%%%%%%%%%%%%%%%%%%%%%%%%%%%%%%%%%%%%%%%%%%%%%%%%%%%%%%
elseif strcmp(text(i,7),'208H1')==1

    %%%%%%%%%%%%%%%%%%%%%%%%%%%%%%%%%%%%%%%%%%%%%%%%%%%%%%%%%%%%%%%%%%%%%%%%%
    if strcmp(text(i,22),'A to B')==1
        H10(i,1)=1;
    elseif strcmp(text(i,22),'B to C')==1
        H10(i,1)=2;
    elseif strcmp(text(i,22),'C to D')==1
        H10(i,1)=3;
    elseif strcmp(text(i,22),'D to E')==1
        H10(i,1)=4;
    elseif strcmp(text(i,22),'>E')==1
        H10(i,1)=5;
    end

```

```

        H10(i,1)=5;
    else
        disp('Error')
    end

    %%%%%%%%%%%%%%%%%%%%%%%%%%%%%%%%%%%%%%%%%
elseif strcmp(text(i,7),'224H1')==1

    %%%%%%%%%%%%%%%%%%%%%%%%%%%%%%%%%%%%%%%%%
    if strcmp(text(i,22),'A to B')==1
        H11(i,1)=1;
    elseif strcmp(text(i,22),'B to C')==1
        H11(i,1)=2;
    elseif strcmp(text(i,22),'C to D')==1
        H11(i,1)=3;
    elseif strcmp(text(i,22),'D to E')==1
        H11(i,1)=4;
    elseif strcmp(text(i,22),'>E')==1
        H11(i,1)=5;
    else
        disp('Error')
    end
    %%%%%%%%%%%%%%%%%%%%%%%%%%%%%%%%%%%%%%%%%

elseif strcmp(text(i,7),'243H1')==1
    %%%%%%%%%%%%%%%%%%%%%%%%%%%%%%%%%%%%%%%%%
    if strcmp(text(i,22),'A to B')==1
        H12(i,1)=1;
    elseif strcmp(text(i,22),'B to C')==1
        H12(i,1)=2;
    elseif strcmp(text(i,22),'C to D')==1
        H12(i,1)=3;
    elseif strcmp(text(i,22),'D to E')==1
        H12(i,1)=4;
    elseif strcmp(text(i,22),'>E')==1
        H12(i,1)=5;
    else
        disp('Error')
    end
    %%%%%%%%%%%%%%%%%%%%%%%%%%%%%%%%%%%%%%%%%

    else
        disp('Error in hinge text')
    end
end

H1=H1 (H1~=0);H2=H2 (H2~=0);H3=H3 (H3~=0);H4=H4 (H4~=0);H5=H5 (H5~=0);H6=H6 (H6~=0);
H7=H7 (H7~=0);H8=H8 (H8~=0);H9=H9 (H9~=0);H10=H10 (H10~=0);H11=H11 (H11~=0);H12=H12
(H12~=0);
Results_Hinges=zeros(size(H1,1),12);

%removing 1st 3 useless rows from text matrix
F_txt(1,:)=[];
F_txt(1,:)=[];
F_txt(1,:)=[];

%extracting the shear at the first 2 piles (frames 26 (V1) and 224 (V2z))
at each limit state
clear V1; clear V2;
for q=1:size(F,1)
    if strcmp(F_txt(q,1),'224')==1
        V1(q,1)=F(q,7);
    elseif strcmp(F_txt(q,1),'26')==1
        V2(q,1)=F(q,7);
    end
end

```



```

    end
end
%removing zeros indecies
V1(V1==0) = [];
V2(V2==0) = [];
%removing repeated numbers (at different stations)
V1=unique(V1,'stable');
V2=unique(V2,'stable');

%OLE
for s=1:size(H1,1)
    if H1(s,1)>=3
        VH1_OLE(1,v)=V1(s,1);
        break
    end
end
for s=1:size(H2,1)
    if H2(s,1)>=3
        VH2_OLE(1,v)=V2(s,1);
        break
    end
end
%CLE
for s=1:size(H2,1)
    if H1(s,1)>=4
        VH1_CLE(1,v)=V1(s,1);
        break
    end
end
for s=1:size(H2,1)
    if H2(s,1)>=4
        VH2_CLE(1,v)=V2(s,1);
        break
    end
end
%DE
for s=1:size(H2,1)
    if H1(s,1)>=5
        VH1_DE(1,v)=V1(s,1);
        break
    end
end
for s=1:size(H2,1)
    if H2(s,1)>=5
        VH2_DE(1,v)=V2(s,1);
        break
    end
end
end

%Extracting displacements of node 422 at different steps
clear d_422_i
clear d_422
for r=1:size(rawT,1)
    if strcmp(rawT(r,1),'422')==1
        d_422_i(r,1)=rawT(r,6);
    else
        d_422_i(r,1)={0};
    end
end
d_422_i=cell2mat(d_422_i);
d_422_i=d_422_i(d_422_i~=0);

d_422(:,v)=d_422_i;

```

```

Results_Hinges(:,1:12)=[H1 H2 H3 H4 H5 H6 H7 H8 H9 H10 H11 H12];

for s=1:size(H1,1)
    if any(Results_Hinges(s,*)>=3)==1
        disp_OLE(1,v)=d_422(s,v);
        break
    end
end

for s=1:size(H1,1)
    if any(Results_Hinges(s,*)>=4)==1

        disp_CLE(1,v)=d_422(s,v);

        break
    end
end

for s=1:size(H1,1)
    if any(Results_Hinges(s,*)>=5)==1

        disp_DE(1,v)=d_422(s,v);

        break
    end
end

M_max_pos(v,1)=max((F(:,12)));
M_max_neg(v,1)=min((F(:,12)));

V_max_pos(v,1)=max((F(:,7)));
V_max_neg(v,1)=min((F(:,7)));
end

histogram(disp_OLE)

save('disp_OLE','disp_OLE')
save('disp_CLE','disp_CLE')
save('disp_DE','disp_DE')

save('VH1_OLE','VH1_OLE')
save('VH1_CLE','VH1_CLE')
save('VH1_DE','VH1_DE')

save('VH2_OLE','VH2_OLE')
save('VH2_CLE','VH2_CLE')
save('VH2_DE','VH2_DE')

Disp_x1g=zeros(Simulations,1);
Disp_x2g=zeros(Simulations,1);
Disp_x3g=zeros(Simulations,1);

%Running and extracting El-Centro demand results

```

```

for v=72:86
    command=sprintf("G:\\SAP2000\\SAP2000.EXE" "G:\\Thesis
Main\\modeling\\The Final Code\\Output_%d.$2k" /R /C',v);
    dos(command)

    %Reading xls output file

    [numT]=xlsread('Results.xls','Joint Displacements - Absolute');
    FileName=sprintf('Results_%d.xls',v);
    copyfile ('Results.xls',FileName)

        Disp_x1g(v,1)=numT(1274,1);
        Disp_x2g(v,1)=numT(1276,1);
        Disp_x3g(v,1)=numT(1278,1);
end

save('Disp_x1g','Disp_x1g')
save('Disp_x2g','Disp_x2g')
save('Disp_x3g','Disp_x3g')

histogram(V_max_pos)
histogram(V_max_neg)
histogram(M_max_pos)
histogram(M_max_neg)
histogram(disp_OLE)
histogram(disp_CLE)
histogram(disp_DE)

%probability of exceedence
c=0;
for i=1:1000
    if abs(y5Disp_2g(i,1)*1.5)>=abs(y5disp_OLE(1,i))
        c=c+1;
    end
end
pf=(c/1000)*100

```

